

COAGULATION OF COLLOIDAL PARTICLES IN TURBULENT FLOWS WITH
APPLICATIONS IN WASTEWATER TREATMENT

by

Michael Angelis Delichatsios

Diploma in Mechanical Engineering
National Technical University of Athens
(1967)

S. M., Massachusetts Institute of Technology
(1971)

SUBMITTED IN PARTIAL FULFILLMENT

OF THE REQUIREMENTS FOR THE

DEGREE OF DOCTOR OF

PHILOSOPHY

at the

Massachusetts Institute of
Technology

September, 1974, *i.e.* Feb, 1975

Signature of Author

Department of Mechanical Engineering

July 25, 1974

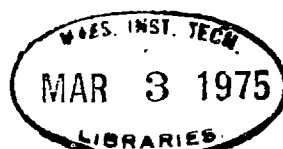
Certified by

Thesis Supervisor

Accepted by

Chairman, Departmental Committee

on Graduate Students



COAGULATION OF COLLOIDAL PARTICLES IN TURBULENT FLOWS WITH
APPLICATIONS IN WASTEWATER TREATMENT

by

Michael Angelis Delichatsios

Submitted to the Department of Mechanical Engineering on July 25, 1974,
in partial fulfillment of the requirements for the degree of Doctor of
Philosophy.

ABSTRACT

The coagulation of colloidal particles of various sizes in a locally isotropic turbulent flow has been investigated theoretically and experimentally. A simple kinetic model for the collision between particles proves to be successful in predicting the coagulation rate of surface charge free colloidal particles. Retardation of coagulation rates by the interparticle repulsive potential is also discussed. The coagulation rate of latex particles is measured inside a fully developed turbulent pipe flow. Finally, a new approach to wastewater treatment systems employing coagulation is proposed, based on a detailed understanding of the interaction between coagulation, breakup, and sedimentation.

Thesis Supervisor: Ronald F. Probst
Title: Professor of Mechanical Engineering

TABLE OF CONTENTS

	Page
TITLE PAGE	1
ABSTRACT	2
ACKNOWLEDGMENTS	3
TABLE OF CONTENTS	4
NOMENCLATURE	6
1. INTRODUCTION	10
2. THEORY FOR THE COAGULATION OF COLLOIDAL PARTICLES IN TURBULENT FLOWS	15
2.1 Coagulation as a Two-step Process	15
2.2 A Simple Kinetic Model for Fully Destabilized Dispersions	18
2.3 Monodisperse Systems	19
2.4 Polydisperse Systems	22
2.5 Comparison of Turbulent Coagulation Rates with Brownian and Shear Flow Coagulation Rates	26
2.6 Turbulent Coagulation in Partially Destabilized Systems	28
3. EXPERIMENTAL DESIGN AND APPARATUS	32
3.1 Purpose of the Experiment and General Description	32
3.2 Flow System	32
3.3 Injection Stations	34
3.4 Sampling Stations	35
3.5 Particle Number Density Analysis	37
3.6 Choice of Dispersed Particles	39
3.7 Preparation and Destabilization of the Latex Polymer Emulsion	39
3.8 Experimental Procedure	41

ACKNOWLEDGMENTS

I would like to express my sincere thanks to my advisor, Professor R. F. Probst, for suggesting to me the subject of the present thesis and for his criticisms during the course of this research. I would also like to thank the other members of my thesis committee, Professor A. A. Sonin of Massachusetts Institute of Technology and Professor L. A. Spielman of Harvard University, for their helpful advice and suggestions. I would like also to express my gratitude to the other members of the Fluid Mechanics Laboratory, who have helped with this thesis, both with their ideas and with their criticisms. Finally, I would like to thank Miss Margaret Gazan for typing a first draft of this thesis and Miss Lucille Blake for typing the final text.

This research was supported by the Office of Naval Research.

	Page
4. PRESENTATION AND DISCUSSION OF RESULTS	42
4.1 Characteristics of Turbulent Pipe Flow	42
4.2 Brownian Coagulation Rate and Particle Surface Potential	43
4.3 Turbulent Coagulation Rate Experiments	45
5. BREAKUP OF DISPERSED PARTICLES IN ISOTROPIC TURBULENT FLOWE	51
6. SCALING LAWS AND APPLICATIONS IN WASTEWATER TREATMENT SYSTEMS	58
6.1 Scaling Laws	58
6.2 A New Approach to Wastewater Treatment	60
7. CONCLUSIONS AND RECOMMENDATIONS	63
APPENDIX A - Limits of the Polydisperseness Coefficient $A(t)$	65
APPENDIX B - The Stability Factor in Brownian Motion Coagulation	67
APPENDIX C - Shipboard Wastewater Treatment	70
REFERENCES	73
TABLES	78
FIGURE TITLES	80
FIGURES	82
BIOGRAPHICAL NOTE	106

NOMENCLATURE

$A(t)$	polydisperseness coefficient for coagulation (dimensionless), Equation (2-31)
b	volume Brownian coagulation rate (cm^3/sec)
d	particle diameter (cm)
D_p	pipe diameter (cm)
D_T	tank diameter (cm)
D_{eff}	effective turbulent diffusion coefficient of the relative particle motion (cm^2/sec)
f	pipe friction coefficient (dimensionless)
$f(\mu_d/\mu)$	function depending on the continuous and dispersed phase viscosities (dimensionless), Equation (5-2)
F	fluid mechanical force acting on a particle (dyn)
g	gravitational acceleration (cm/sec^2)
G	rate of strain in shear flows (sec^{-1})
H	Hamaker constant (ergs)
k	Boltzmann constant (ergs/ $^{\circ}\text{K}$)
ℓ	turbulent coagulation pipe length (cm)
L	Eulerian macroscale of turbulence (cm)
$n(v, t)$	particle volume distribution (cm^{-6})
N	total particle number density (cm^{-3})
$p(u)$	probability distribution function of the relative velocity u
$p(\dot{u})$	probability distribution function of the relative acceleration \dot{u}

$p(u, \dot{u})$	joint probability distribution function between the relative velocity u and acceleration \dot{u}
P	impeller power input in an agitator tank (ergs/sec)
Q	pipe flow rate (gpm)
r	distance between two points (cm)
r_o	maximum distance of potential action from the center of a particle (cm)
Re	pipe Reynolds number $(\frac{U D}{\nu} P)$
t	time (sec)
T	absolute temperature ($^{\circ}K$)
u	turbulent relative velocity between two points (cm/sec)
u_1	instantaneous turbulent velocity at a point (cm/sec)
u_b	breakup characteristic velocity (cm/sec)
u_c	cutoff velocity value of the relative velocity probability distribution function (cm/sec)
u_D	induced relative velocity by potential forces (cm/sec) Equation (2-46)
u_k	Kolmogorov characteristic velocity (cm/sec), Equation (2-12)
u_r	root mean square relative particle velocity (cm/sec)
$(u_r)_{eff}$	effective collision velocity in partially destabilized systems (cm/sec), Equation (2-47)
u_s	particle settling velocity (cm/sec)
$\frac{u_*}{(u'^2)^{1/2}}$	pipe friction velocity (cm/sec), Equation (4-2)
	root mean square turbulent velocity at a point (cm/sec)
\dot{u}	turbulent relative acceleration between two points (cm/sec ²)

$\overline{(\dot{u}^2)}^{1/2}$	root mean square turbulent relative acceleration between two points (cm/sec ²), Equations (5-10), (5-11)
U	average pipe velocity (cm/sec)
v	particle volume (cm ³)
V _r	tank volume (cm ³)
W(r)	interparticle potential energy as a function of the distance between the particle centers (ergs)
W _o	characteristic interparticle potential energy (ergs)
W _{Br}	Brownian coagulation stability factor (dimensionless)
W _{turb}	turbulent coagulation stability factor (dimensionless)
x	distance from the first sampling station along the pipe (cm)

Greek Symbols

γ	drop surface tension (dyn/cm)
ε	rate of turbulent energy dissipation per unit mass (ergs/sec. gm)
η	ratio of shear flow to turbulent transport (dimensionless)
θ	temperature (°C)
λ	Kolmogorov microscale of turbulence (cm)
λ _D	Debye length (cm)
μ	viscosity of the continuous phase (gm/sec.cm)
μ _d	viscosity of the dispersed phase (gm/sec.cm)
ν	kinematic viscosity of the continuous phase (cm ² /sec)
ξ	dimensionless particle volume, Equation (2-25)
ρ	density of the continuous phase (gm/cm ³)
ρ _p	particle density (gm/cm ³)
σ	strength of the particle material to deformation (dyn/cm ²)

τ	Kolmogorov time scale (sec), Equation (2-5)
τ_b	breakup characteristic time (sec), Equations (5-13), (5-14)
τ_{Br}	Brownian coagulation characteristic time (sec), Equation (2-35)
τ_c	turbulent coagulation characteristic time (sec) Equation (2-36)
τ_d	turbulent characteristic time in the inertial subrange (sec), Equation (2-6)
τ_r	particle motion relaxation time (sec), Equation (2-4)
ϕ	volume fraction of the dispersed phase (dimensionless)
ϕ_D	destabilizer volumetric concentration (dimensionless)
$\psi(\xi, t)$	dimensionless particle size distribution, Equation (2-26)
ω	particle coagulation rate in a fully destabilized system (sec^{-1})
$\omega_b(v)$	breakup rate of a particle with volume v (sec^{-1})
ω_D	particle coagulation rate in a partially destabilized system (sec^{-1})
ω_{1F}	coagulation rate of primary particles with flocs (sec^{-1})
$\omega(v, v')$	volume swept per unit time during collision between particles of volumes v and v' (cm^3/sec)

1. INTRODUCTION

Systems of particles dispersed in a continuous phase are very common in practice. They are usually known as aerosols, dispersions of particles in a gaseous medium, suspensions, dispersions of solid particles in a liquid medium, and emulsions, dispersions of drops in a liquid medium.

In many applications the coagulation between the dispersed particles is of major importance with respect to the treatment, handling, or behavior of the dispersions. In this work we are mainly going to consider dispersions of colloidal particles in a liquid medium.

Colloidal particles of submicron or micron size acquire a surface charge, usually negative. The dispersions of these particles in a liquid medium remain stable for a long time, since both the gravitational forces are weak compared to thermal motion, and coagulation of the particles is inhibited due to interparticle potential repulsions.

It is apparent that coagulation is a two-step process. Kinetic transport leads to particle collisions, and aggregation between two particles is accomplished as soon as the interparticle repulsive action is overcome. Particle transport may take place as a consequence of Brownian motion, shear flow, and turbulent agitation. The shielding action of the surface charge can be reduced or neutralized, i.e., the dispersion is destabilized, by the addition of chemicals dissolved in the dispersion.

The destabilization of the dispersion by the chemicals may be accomplished in four distinct ways (O'Melia in Weber (1972)):

1. Adsorption of the chemicals on the particle's surface
for charge neutralization

2. Adsorption for particle bridging
3. Entrapment of particles in metal hydroxide precipitate
4. Repression of the effective range of the interparticle potential.

The phenomenon of coagulation has been analyzed in a large number of works. Smoluchowski (1916) developed successful theories for the coagulation of surface charge free particles in Brownian motion and shear flow. He assumed that particle interactions at short distances can be neglected. Saffman and Turner (1956) and independently Levich (1962) developed models for the coagulation in isotropic turbulent flows of surface charge free dispersed particles of size less than the Kolmogorov microscale.

In parallel Fuchs (1934) incorporated in Smoluchowski's diffusion model for the Brownian coagulation between charged particles the effects of interparticle repulsions.

In late 1940's the now generally accepted VODL (Verwey-Overbeek and Derjaguin-Landau) theory succeeded in relating the particle surface charge and the interparticle repulsive potential to the physiochemical properties of a whole class of dispersions, the lyophobic dispersions (see, e.g., Verwey-Overbeek (1948)). Using the theory developed by Fuchs (1934), Reerink and Overbeek (1954) estimated the retardation effects of the repulsive action on the Brownian coagulation rates.

Finally the viscous interactions between particles at short distances were incorporated in Smoluchowski's theory for Brownian coagulation by Spielman (1970).

Numerous experimental investigations verified Smoluchowski's theory for Brownian and shear flow coagulation (see more references in Swift and Friedlander (1964)). The agreement of the experimental results with these theories indicates that in many cases the viscous interaction effects suggested by Spielman (1970) may be neglected.

Several experiments in agitator tanks (see, e.g., Birkner and Morgan (1968) and Hahn and Stumm (1968)) failed to completely verify the existing theories of turbulent coagulation. In these experiments not completely destabilized dispersions were used. Moreover, the turbulent flow inside an agitator tank is far from homogeneous and isotropic (Lattke (1971)), a basic assumption in the theories of turbulent motion coagulation suggested by Saffman and Turner (1956) and Levich (1962).

Finally it is important to notice here that for deformable particles, for example, drops with size larger than the colloidal particles, the squeezing of the continuous phase film between the particles during collision may have a significant influence on their coagulation. This has already been observed in Brownian coagulation experiments (Tempel (1953)). We expect that due to the higher interparticle collision forces the squeezing effect will be negligible in turbulent coagulation.

In this thesis we develop a new theory, based on simple kinetic theory collision concepts, for the turbulent coagulation of dispersed particles of sizes less than or larger than the Kolmogorov microscale. Partially destabilized systems are also included in this analysis. Experiments in fully developed turbulent pipe flows have been carried out, and the experimental results are compared with the theoretical predictions. The ultimate

goal is the rational design of wastewater treatment systems after complete knowledge of the coagulation phenomenon has been gained.

During the course of this work it became apparent that breakup of particles under turbulent conditions posed a limit in the operation of wastewater treatment systems employing coagulation. The maximum particle size in dilute dispersions under known turbulent flow conditions is well predicted by the theories of Kolmogorov (1949) and Hinze (1955), for particles with size in the inertial subrange of an isotropic turbulent flow. In dense dispersions coagulation opposes breakup, and a steady average particle size is reached when the coagulation rate is equilibrated to the breakup rate. A new model is suggested in this work for the estimation of the breakup rate of particles in isotropic turbulent flows.

Important scaling laws relating coagulation, breakup, and sedimentation of particles are developed based on the knowledge gained in this whole work. A new method and apparatus for wastewater treatment in ships is finally proposed with the great advantage of considerably reducing the space requirements by making use of existing piping.

An outline of the contents of this dissertation illustrates in general the approach used in this research. Chapter 2 contains the theoretical models of turbulent coagulation for fully or partially destabilized systems with dispersed particles of various sizes in comparison with the Kolmogorov microscale. The experimental set-up and procedure to measure the coagulation rate between particles in turbulent pipe flows are described in Chapter 3. In Chapter 4 the experimental results are analyzed and compared

with the theoretical predictions. Breakup rates of particles and their maximum size in an isotropic turbulent flow is discussed in Chapter 5. Scaling laws pertinent to wastewater treatment systems and a new method for wastewater treatment are brought forward in Chapter 6. Finally, some important recommendations for continuation of the present work are given in Chapter 7.

2. THEORY FOR THE COAGULATION OF COLLOIDAL PARTICLES IN TURBULENT FLOWS

2.1 Coagulation as a Two-step Process

As it has been pointed out in the introduction coagulation is a two-step process, namely, kinetic transport of particles leading to eventual collisions and sticking of the particles to form one particle after the interparticle repulsion is overcome. The collision rate between particles depends on their relative velocity, their size and particle size distribution, and the particle number density, that is, the number of particles per unit volume of the continuous phase. The probability of sticking will depend primarily on the intensity of interparticle potential energy and the hydrodynamic forces during collision available to counteract this potential.

It is proposed that turbulent motion may increase the coagulation rate in comparison with shear flow or Brownian motion by two factors. Higher relative velocities lead to an increase of the collision rate, while at the same time greater impact energies during collisions may improve the sticking probability of particles.

Before going further in the investigation of the coagulation between particles in isotropic turbulent flows, we put forward the assumptions underlying the present analysis.

1. Only isotropic turbulent flows will be considered here. This is not really a severe restriction because many turbulent flows may be modeled as locally isotropic.
2. Binary collisions will take place during particle interactions; that is, only dilute dispersions will be studied. For homogeneous

dispersions with a volume fraction of the dispersed phase ϕ , this assumption will be applicable if $\phi^2 \ll 1$. Here ϕ^2 can be interpreted as the probability that two particles are found simultaneously at a distance of a particle diameter from a third particle (Batchelor (1972)).

3. Gravitational forces may be in general neglected when the particle settling velocity is much smaller than the root mean square turbulent velocity (Owen (1969)).

The settling velocity is equal to (Owen (1969)),

$$u_s = \frac{1}{18} \frac{\rho_p - \rho}{\rho} \frac{gd^2}{\nu} . \quad (2-1)$$

Here ρ_p is the particle density, d its diameter, ρ the density and ν the kinematic viscosity of the continuous phase.

The root mean square turbulent velocity is given (Batchelor (1960)) by

$$\overline{(u')^2}^{1/2} = (\epsilon L)^{1/3} \quad (2-2)$$

where ϵ is the rate of turbulent energy dissipation per unit mass, and L is the Eulerian macroscale of turbulence.

It follows that gravitational effects will be negligible when

$$\frac{u_s}{\overline{(u')^2}^{1/2}} \ll 1 . \quad (2-3)$$

4. Due to strong interparticle impact forces, the squeezing of the continuous phase film during collision between two particles will not be an important factor in turbulent coagulation. Moreover, its

significance is minimal in the coagulation of dispersed colloidal size nondeformable particles even in the case of Brownian motion.

5. Interactions between two particles will be neglected. Interactions between particles and the continuous phase will be small for dilute systems.

There is no comprehensive analysis of particle interactions at short interparticle distances in an isotropic turbulent flow, in analogy, for example, to the Stokes flow particle interactions (Batchelor (1972)). Owen (1969) has estimated that in a dispersion the rate of turbulent energy dissipation per unit mass compared with that of a particle free continuous fluid is increased by a factor of $(1 + \phi)$.

6. Slip velocities between a particle and the continuous phase will be insignificant if the relaxation time of the particle motion is less than a turbulent characteristic time.

For spherical particles and relative velocities such that the Reynolds number of the particle motion is less than one, the relaxation time is (Owen (1969)),

$$\tau_r = \frac{1}{18} \frac{(\rho_p + \rho/2)}{\rho} \frac{d^2}{\nu} \quad (2-4)$$

The turbulent characteristic time is that of an eddy of size equal to the particle diameter. For particles with size less than the Kolmogorov microscale ($\lambda = (\frac{\nu^3}{\epsilon})^{1/4}$), this time is equal to the Kolmogorov time scale (Rotta (1972)).

$$\tau = \left(\frac{\nu}{\epsilon}\right)^{1/2} . \quad (2-5)$$

For particles with size in the inertial subrange of turbulence, the turbulent characteristic time is (Rotta (1972)),

$$\tau_d = \frac{d}{(\epsilon d)^{1/3}} \quad (2-6)$$

Thus slip velocities will be neglected when

$$\frac{\tau_r}{\tau} \ll 1 \quad \text{for } d < \lambda \quad (2-7)$$

$$\frac{\tau_r}{\tau_d} \ll 1 \quad \text{for } d > \lambda. \quad (2-8)$$

These conditions are in general satisfied for colloidal particles dispersed in a liquid medium.

7. Finally, breakup of colloidal size particles does not take place under normal turbulent flow conditions. This statement will be justified in greater detail in Chapter 5.

2.2 A Simple Kinetic Model for Fully Destabilized Dispersions

In what follows we assume that the dispersion is fully destabilized; namely, the interparticle potential forces are neutralized by the addition of chemicals called coagulants or coagulant aids (Weber (1972)). The coagulation rate of particles will then be effectively equal to their collision rate.

In his pioneering work Smoluchowski (1916) suggested a simple diffusion model for Brownian coagulation. Each particle is considered as a potential coagulating sphere towards which the surrounding particles diffuse and subsequently coagulate. This model has been lately corrected by Spielman (1970) to take into account viscous interactions between the particles. A simple collision model developed by Smoluchowski (1917)

predicts that the coagulation rate of particles in a shear flow is proportional to the rate of strain.

Camp and Stein (1943) suggested that the same result for shear flow coagulation could be used in estimating the coagulation of particles inside turbulent agitators. The rate of strain should be replaced by $(\epsilon/\nu)^{1/2}$.

Saffman and Turner (1956) calculated the coagulation rate in turbulent clouds of drops with sizes less than the Kolmogorov microscale by analyzing the flow field around a drop. They found the same functional form for the coagulation rate as that suggested by Camp and Stein (1943) with a different proportionality constant.

Finally, Levich (1962) extended the Brownian diffusion model in turbulent motion coagulation and estimated the coagulation rate of colloidal particles. His results agree with the predictions of previous investigators, but the proportionality constant is approximately one order of magnitude larger. This discrepancy may be attributed to the inability of a steady diffusion model to correctly describe the relative particle motion in turbulent flows due to the non-Markovian nature of the turbulent dispersion process.

In this work we propose a simple kinetic model for the coagulation between particles in isotropic turbulent flows that accounts for the statistical nature of particle transport. This model can predict the coagulation rate between particles of various sizes in an isotropic turbulent flow.

2.3 Monodisperse Systems

In order to better understand the physics, we consider here a dispersion consisting of equal size spherical particles in a liquid medium.

According to simple kinetic theory concepts, the volume swept by a particle per unit time in a collision between particles is

$$\omega(v,v) = \pi d^2 u_r . \quad (2-9)$$

Here u_r is the root mean square relative particle velocity during collision, v is the volume of each particle, and (πd^2) is the collision cross section.

The coagulation rate between particles will be given by

$$\omega = 1/2 \omega(v,v) N \quad (2-10)$$

where N is the number particle density, and the factor $1/2$ ensures that each collision is counted only once.

It follows that the variation of the particle number density with time will be

$$\frac{dN}{dt} = - \omega N . \quad (2-11)$$

The relative turbulent velocity introduced in Equation (2-9) is a function of the distance between particles during collision. It is equal to the square root of the second-order correlation of the turbulent velocity difference between two points at a distance of a particle diameter in an isotropic turbulent flow. The second-order correlation of the turbulent velocity difference between two points is calculated from Kolmogorov's similarity theory (Rotta (1972)), and it is depicted in Figure 1. In this figure $(u_1 - u_1')$ is the difference of the turbulent velocity components at two points at an arbitrary distance r along the vector joining the two points. The characteristic velocity implied in this figure is the Kolmogorov characteristic velocity

$$u_k = (\epsilon \nu)^{1/4} . \quad (2-12)$$

The Eulenan macroscale of turbulence L is taken one thousand times larger than the Kolmogorov microscale λ .

The relative velocity between particles during collision, u_r , can now be approximated by

$$u_r \approx \left(\overline{(u_1 - u'_1)^2} \right)_{r=d}^{1/2} . \quad (2-13)$$

It is not possible to calculate the exact value of u_r . We may assume that each cartesian component of the relative velocity between two points in isotropic turbulence has a Gaussian probability distribution. This is approximately corroborated from the experiments by Townsend (1947) and Van Atta and Park (1972). If we further assume that the turbulent relative velocity components between two points are statistically independent, we may find, using methods similar to classical gas kinetic theory, that the relative particle velocity is equal to the value given in Equation (2-13) multiplied by a factor $2\sqrt{2/\pi} = 1.59$. Since the relative velocity components can never be considered statistically independent (Rotta (1972)), and since we cannot account for the exact velocity distribution functions, we use in what follows the approximate expression of Equation (2-13) in evaluating the coagulation rates.

Thus from Equation (2-10) and using Equation (2-13) and the results depicted in Figure 1, we find after some rearrangements that the coagulation rate is

$$\frac{\omega \tau}{\phi} = 0.77 \quad \text{for } d \lesssim \lambda \quad (2-14)$$

$$\frac{\omega\tau}{\phi} = 4.11(\lambda/d)^{2/3} \quad \text{for } d > \lambda \quad (2-15)$$

$$\frac{\omega\tau}{\phi} = 3\left(\frac{L}{\lambda}\right)^{1/3} \lambda/d \quad d \sim L \quad (2-16)$$

In the above equations the volume fraction of the dispersed phase is

$$\phi = \pi/6 d^3 N \quad (2-17)$$

The results given by Equations (2-14), (2-15), and (2-16) are plotted in Figure 2. In this plot $L = 10^3 \lambda$.

In many practical applications the size of colloidal particles is less than the Kolmogorov microscale, and Equation (2-14) is applicable. For example, in order to have $\lambda = 10\mu\text{m}$ the required rate of turbulent energy dissipation per unit mass in an aqueous dispersion is

$$\epsilon = \frac{v^3}{\lambda^4} = 10^6 \quad \text{erg/sec} \cdot \text{gm} \quad (2-18)$$

This corresponds to a practically tremendous energy input.

Finally, Equation (2-15) will be applicable only in cases when an inertial subrange of turbulence exists, namely, when $L \gg \lambda$ (Rotta (1972)).

2.4 Polydisperse Systems

It is straightforward to write a kinetic equation for the change of the particle number density with time in a polydisperse two-phase system. This has already been done by previous investigators for Brownian motion and shear flow (see, e.g., Swift and Friedlander (1964)).

We assume the particle size distribution to be given by a continuous function $n(v,t)$, so that $n(v,t) \Delta v$ be the number of particles per unit volume of the continuous phase at time t with volumes between v and $v + \Delta v$.

Let also $\omega(v, v')$ be the volume collision frequency between particles with volumes v and v' , that is, the volume swept per unit time in their relative motion during collision.

Then in similarity to Equation (2-9) and in accordance with our simple kinetic model

$$\omega(v, v') = \pi \left(\frac{d + d'}{2} \right)^2 u_r \quad (2-19)$$

Here d, d' are the diameters of particles of volumes v and v' , respectively. The relative velocity introduced in Equation (2-19) will be equal to

$$u_r = \overline{((u_1 - u'_1)^2)}^{1/2} \quad (2-20)$$

$$r = \frac{d + d'}{2}$$

Following previous experience (Swift and Friedlander (1964)), the evolution of the particle size distribution with time is

$$\frac{dn(v, t)}{dt} = 1/2 \int_0^v \omega(v', v - v') n(v', t) n(v - v', t) dv' - \int_0^v \omega(v, v') \cdot n(v, t) n(v', t) dv' \quad (2-21)$$

To write this equation we have made use of the assumptions that only binary collisions take place, and no breakup of particles is probable.

The total particle number density is

$$N = \int_0^\infty n(v, t) dv \quad (2-22)$$

and the volume fraction of the dispersed phase ϕ is

$$\phi = N \bar{v} = \int_0^\infty vn(v, t) dv \quad (2-23)$$

where \bar{v} is the average particle volume.

Integrating Equation (2-21) with respect to v , the change of the total particle density is

$$\frac{dN}{dt} = -\frac{1}{2} \int_0^\infty \int_0^\infty \omega(v, v') n(v, t) n(v', t) dv dv' . \quad (2-24)$$

This equation degenerates to the simpler Equation (2-11) for mono-disperse systems.

Equations (2-21) and (2-24) are quite general for various particle sizes if the appropriate volume collision frequency is selected from Equations (2-19) and (2-20).

Using dimensionless parameters we can simplify Equation (2-24). The proper dimensionless volume and particle size distribution suggested by Swift and Friedlander (1964) are

$$\xi = \frac{vN}{\phi} \quad (2-25)$$

$$\psi(\xi, t) = \frac{\phi}{N^2} n(v, t) . \quad (2-26)$$

The dimensionless particle size distribution satisfies the relations (cf. Equations (2-22) and (2-23))

$$\int_0^\infty \psi(\xi, t) d\xi = 1 \quad (2-27)$$

$$\int_0^\infty \xi \psi(\xi, t) d\xi = 1 . \quad (2-28)$$

It follows that Equation (2-24) may be rewritten using Equations (2-25) and (2-26) as

$$\frac{dN}{dt} = -\frac{1}{2} N^2 \int_0^\infty \int_0^\infty \omega\left(\frac{\xi\phi}{N}, \frac{\xi'\phi}{N}\right) \psi(\xi, t) \psi(\xi', t) d\xi d\xi' . \quad (2-29)$$

Equation (2-29) is further simplified to the form

$$\frac{dN}{dt} = - \omega N A(t) \quad (2-30)$$

where the appropriate volume collision rate $\omega(v, v')$ (Equation (2-19)) has been used. Here ω is the coagulation rate corresponding to a monodisperse system with the same volume fraction of the dispersed phase ϕ , and $A(t)$ is a correction factor due to polydispersity.

For the most important case of colloidal dispersions with particle sizes less than the Kolmogorov microscale, the correction factor $A(t)$ takes the simple form

$$A(t) = \frac{1}{8} \int_0^\infty \int_0^\infty (\xi^{1/3} + \xi'^{1/3})^3 \psi(\xi, t) \psi(\xi', t) d\xi d\xi' . \quad (2-31)$$

Using the following algebraic inequalities

$$(\xi + \xi') < (\xi^{1/3} + \xi'^{1/3})^3 \leq 4(\xi + \xi') , \quad (2-32)$$

it can be proved that

$$0.25 \leq A(t) \leq 1 . \quad (2-33)$$

The correction factor $A(t)$ is equal to one for monodisperse systems, and it will take the minimum value 0.25 for a system consisting of two monodisperse systems with widely differing volume fractions and widely differing particle number densities in the inverse order. An outline of the proof is given in Appendix A.

In general the polydisperseness coefficient $A(t)$ will be a function of time, except for the case the dimensionless particle size distribution is independent of time, namely, when there is a similarity solution for the particle size distribution (Swift and Friedlander (1964)).

In a recent paper (Pulvermacher and Ruckenstein (1974)), it has been proved that such a solution cannot exist for the collision function $(\xi^{1/3} + \xi'^{1/3})^3$ implied in Equation (2-31).

2.5 Comparison of Turbulent Coagulation Rates with Brownian and Shear Flow Coagulation Rates

In the previous two sections it was tacitly assumed that only turbulent coagulation is present or that Brownian or shear flow coagulation are negligible. The conditions for which the latter statement is true are developed in this section.

Turbulent action dominates when the relevant length scale of a phenomenon is much larger than the molecular dimensions. This means that for length scales less than a size, which has to be defined for each phenomenon, Brownian motion resulting from molecular interactions will be solely significant.

In a coagulation process turbulent flow will dominate compared to Brownian motion when the turbulent coagulation time is less than the Brownian coagulation time. In the following analysis we assume a monodisperse and homogeneous dispersion.

The turbulent coagulation time is the inverse of the coagulation rate given in Equation (2-14), and the Brownian coagulation time (Levich (1962)) is

$$\tau_{Br} = \frac{\pi\mu d^3}{8 kT \phi} . \quad (2-34)$$

Here μ is the viscosity of the continuous phase, k the Boltzmann constant, and T the absolute temperature of the dispersion. For a dispersion in water at room temperature ($\theta = 20^\circ \text{C}$),

$$\tau_{Br} = 0.97 \cdot 10^{11} \frac{d^3}{\phi} \quad (2-35)$$

where d has dimensions of cm and τ_{Br} of sec.

The turbulent coagulation time is,

$$\tau_c = 1.30 \frac{\tau}{\phi} \quad , \quad (2-36)$$

and the condition that turbulent coagulation dominates is expressed by the relation

$$\frac{\tau_c}{\tau_{Br}} = \frac{10.4 \text{ kT}}{\pi\mu} \sqrt{\nu/\epsilon} \frac{1}{d^3} \sim 1 \quad . \quad (2-37)$$

For a dispersion in water Equation (2-37) leads to

$$d > 2.37 \cdot 10^{-4} \left(\frac{\nu}{\epsilon}\right)^{1/6} \quad . \quad (2-38)$$

Here d is in cm, ν in cm^2/sec , and ϵ in $\text{erg}/\text{sec} \cdot \text{gm}$.

The interaction between turbulent and shear flow coagulation is very complicated, and a detailed analysis is out of the scope of the present thesis. The coagulation of particles will be affected both by the turbulent fluctuating motion and the local shear flow. The proper dimensionless number which expresses the ratio of shear flow to turbulent transport is

$$\eta = \frac{Gd^2}{D_e} \quad . \quad (2-39)$$

Here G is the local rate of strain of the shear flow, and D_e is an effective turbulent diffusion coefficient of the relative particle motion. The effective turbulent diffusion coefficient is approximately equal to (Levich (1962))

$$D_{\text{eff}} \approx u_r d \approx \sqrt{\epsilon/r}^2 d \quad d < \lambda \quad (2-40)$$

$$D_{\text{eff}} \approx u_r d \approx (\epsilon d)^{1/3} d \quad d > \lambda \quad (2-41)$$

Turbulent coagulation will dominate if the dimensionless group η in Equation (2-39) is less than one. This happens when

$$G < \sqrt{\epsilon/\nu} \quad d < \lambda \quad (2-42)$$

$$d < \left(\frac{\epsilon}{G^3}\right)^{1/2} \quad d > \lambda \quad (2-43)$$

In shear flow turbulence there may be regions where turbulent and shear flow coagulation rates are of the same order of magnitude. There is no reason to expect that turbulent motion and shear flow act independently in promoting the coagulation of particles. In the context of the present discussion it is remarkable to notice that Swift and Friedlander (1964) postulated in their work that Brownian and shear flow coagulation are additive, although this is devoid of any theoretical justification. Further experimental and theoretical work to study the coagulation of particles in shear flow turbulence would be valuable.

2.6 Turbulent Coagulation in Partially Destabilized Systems

The statistical analysis of the previous sections has provided a method for calculating the collision frequency between particles in a turbulent flow. It does not seem possible to extend this method rigorously so that effects of interparticle potential repulsion are incorporated. The basic reason is that it is not feasible to describe the interaction between particles in any detailed fashion, when potential forces are present.

An alternative method would be to use a diffusion model to describe the coagulation and then follow the analysis suggested by Fuchs (1934) to incorporate in it interparticle potential effects. Levich (1962) proposed a diffusion model for turbulent coagulation in fully destabilized systems. Although his results agree with Equation (2-14), except for the proportionality constant, the proposed diffusion equation is not theoretically justified. The underlying reason is that the relative dispersion of particles in turbulent flows is not a Markovian process, and the characteristic diffusion length scale has a wide spectrum from eddies of a particle diameter to the macroscale of turbulence (see Batchelor and Townsend (1956) and Roberts (1961)).

In a coagulation process of partially destabilized dispersed particles, the coagulation is accomplished in the following way. Particles are transported by turbulent motion near another particle. For short interparticle distances the repulsive potential slows down the particle relative motion, and only a fraction of incoming particles succeeds in coagulating with another particle.

The interparticle potential energy can be characterized by a characteristic value W_o acting over a distance λ_D from the particle surface. The characteristic value W_o may be taken typically equal to the maximum interparticle potential energy, while λ_D will be of the order of the Debye length (Overbeek (1952)).

Based on dimensionless arguments it is seen that the retarded coagulation rate for a monodisperse system will have the form

$$\omega_D = \omega_{fcn} \left(\frac{\lambda_D}{d}, \frac{W_o}{\lambda_D F} \right) . \quad (2-44)$$

Here ω is the coagulation rate of particles in a system fully destabilized, and F is the fluid mechanical force on a particle. For particles of size less than the Kolmogorov microscale, the fluid mechanical force is

$$F \approx 3\pi\mu d u_r \quad (2-45)$$

where u_r is the relative particle velocity (see Equation 2-9)), and the approximate sign in Equation (2-45) implies that the fluid mechanical forces may be reduced due to particle-particle interactions.

An estimate of the functional relation in Equation (2-44) for a monodisperse system consisting of particles with size less than the Kolmogorov microscale is obtained in the following way. The relaxation time of the particle motion of micron size colloidal particles (cf Equation (2-4)) is less than the time (λ_D/u_r) a particle would require to move a distance equal to the Debye length, while the Kolmogorov characteristic time of an eddy ($(\nu/\epsilon)^{1/2}$) is much larger. Thus at short interparticle distances and for sufficiently small values of the potential energy W_0 that Stokes flow conditions prevail, a relative velocity will be induced by the potential field

$$u_D = - \frac{W_0}{\lambda_D(3\pi\mu d)} \quad (2-46)$$

It follows that the instantaneous turbulent relative velocity between the particles during collision will be reduced by an amount equal to the induced velocity u_D . Coagulation will take place whenever the instantaneous turbulent relative particle velocity is absolutely larger than u_D . For small values of u_D it can be found that the effective collision velocity will be

$$(u_r)_{\text{eff}} = u_r - u_D . \quad (2-47)$$

Using the simple kinetic model defined in Equation (2-10) with an effective collision cross section diameter $d + \lambda_D = r_o$ and relative particle velocity given by Equation (2-47), we obtain the following expression for the reduced coagulation rate

$$\omega_D = \omega \left(1 + \frac{\lambda_D}{d}\right)^2 \left(1 - \frac{W_o}{3\pi\mu d u_r \lambda_D}\right) . \quad (2-48)$$

Equation (2-47) agrees with the general functional form in Equation (2-44) obtained from dimensionless arguments.

3. EXPERIMENTAL DESIGN AND APPARATUS

3.1 Purpose of the Experiment and General Description

Experiments were carried out in order to measure the coagulation rate of colloidal particles in turbulent flows. The fully developed turbulent flow inside a circular pipe was selected as the ambient flow field because its turbulent characteristics are long ago well known, and the flow is nearly isotropic in the core of the pipe (Laufer (1954)).

Commercially available latex particles were dispersed in water. They were selected because they have a narrow particle size distribution and consist of spherical neutrally buoyant particles.

The variation of the mean particle size and the particle size distribution was obtained by measuring the particle size distribution of samples directly taken along the pipe flow with the Coulter Counter (Wachtel and La Mer (1962)).

The initial particle size and their concentration, the degree of their destabilization, and the pipe flow rate were varied in the course of the present experiments

3.2 Flow System

In designing the flow system the following considerations were taken into account:

1. The pipe flow rate should be constant.
2. The water should be free of interfering contaminants.
3. The flow should be fully developed.
4. Full mixing of the emulsion and the destabilizer with the water in the pipe flow should be ensured before any samples were withdrawn.

5. The length of the pipe should be selected in such a way that a measurable degree of coagulation takes place along the pipe.

A general view of the experimental setup is shown in Figure 3. The flow was established by means of a suitable commercial centrifugal pump. The flow rate was kept constant by virtue of an overflow tank shown in Figure 3. A rotameter, located after the pump, was calibrated to measure the flow rate with accuracy ± 1 per cent of the full scale. The rotameter had a range from 2 gpm to 17 gpm (manufacturer Fisher and Porter).

Two honeycomb filters were used to clean the supply water from foreign particles. Moreover, in order to minimize the quantity of contaminants in the system, all components were carefully cleaned before assembling them. Water was then run through the system for one month before measurements were made. Samples of clean water were regularly withdrawn from the system and analyzed by the Coulter Counter. The measured total number density of particulate matter in water was typically found to be 10^6 particles/cm³, which was four orders of magnitude less than the typical number density of latex particles in an experimental run (approximately 10^{10} particles/cm³). We decided to neglect this correction since the error in measuring the particle number density with the Coulter Counter is higher.

Lucite pipe of 1-inch inside diameter (measured with accuracy of ± 0.5 per cent) and a total length of 24 feet was used in order to have visual observation of the flow. Measurements of the pressure drop inside the above pipe for fully developed turbulent flows showed that the

friction coefficient was the same as the one given by standard frictional resistance curves in smooth pipes (see, e.g., Schlichting (1968)). The inlet pipe length was selected so that fully developed turbulent flow prevails in the test section (see, e.g., Schlichting (1968)). The disturbance of the turbulent flow due to the bends was estimated to be small (see, e.g., Schlichting (1968) note on p. 540).

The pipeline after the position II in Figure 3 was made of five pipe segments of variable length connected together with plastic joints. The ends of these pipe segments were tapered so that smooth fitting with the plastic joints would be insured.

3.3 Injection Stations

The stable latex emulsion was injected into the pipe flow at position I, as it is shown in Figure 3. The emulsion of known concentration was directly released into the pipe from a pressurized tank through a solenoid valve actuated by an electric timer shown in Figure 3. The flow rate of the emulsion from the tank into the pipe flow was calculated by measuring the volume withdrawn from the tank in a specified time interval set by the electric timer. The volume fraction of the dispersed phase in the pipe flow could then be readily calculated.

The destabilizer was released into the pipe flow at position II after complete mixing of the emulsion with the water was ensured. The distance between injection ports I and II was sixty times the pipe diameter, enough length for complete mixing to take place (see Brodkey (1966)).

The injection system for the destabilizer was similar to the one used for the emulsion except for the injection port at II. A special design, shown in Figure 4, was provided to speed up the mixing of the

destabilizer with the pipe flow. The destabilizer was injected at an angle counter to the pipe flow along the circumference of the pipe cross section. Gross visual observations of the mixing process using a dye showed that complete mixing took place in a distance of approximately fifteen pipe diameters. From similar experimental arrangements (see Hartung and Hiby (1972)) it was found that mixing is practically completed at a distance of ten pipe diameters from the injection port. The associated mixing time was always much less (approximately one order of magnitude) than the characteristic coagulation time. Thus the effects of inhomogeneous mixing of the destabilizer with the pipe flow could be neglected.

3.4 Sampling Stations

Samples from the pipe were withdrawn at five stations along the pipe shown in Figure 3. A sketch of a typical station is shown in Figure 5.

Withdrawal of the dispersion from the pipe was obtained through a copper pipette (1/4-inch inside diameter and 1-inch length) starting from the pipe wall. The sample was directly diluted in a 1-liter glass flask containing water twice filtered. A solenoid valve at each station controlled the withdrawal time, typically less than one second. The quantity withdrawn was measured by collecting the displaced water from the flask in a beaker located after the solenoid valve. Mild mixing of the sample entering the flask was provided by a magnetic stirrer shown in Figure 5.

The following problems were looked at when the sampling stations were designed:

1. The degree of coagulation of the emulsion in the sample during the flow inside the copper pipette was estimated to be less than 1 per cent of the particle number density. For a typical experiment the velocity inside the pipette was 500 cm/sec. This velocity was calculated by measuring the quantity withdrawn in a certain time interval at a sampling station. The associated characteristic time for coagulation was estimated 0.4 sec for a typical dispersion with volume fraction $\phi = 10^{-3}$, while the flow time through the pipette was $5 \cdot 10^{-3}$ sec. It follows that the degree of coagulation in the pipette could be neglected inasmuch as the error in the measurement of the particle number density with the Coulter Counter is larger (± 3 per cent).
2. By diluting the sample directly in the 1-liter flask, further coagulation of the dispersed phase by Brownian motion was minimized. The corresponding Brownian coagulation time was very large because the emulsion was very dilute in the flask ($\phi \approx 10^{-5}$), and the concentration of the destabilizer was simultaneously lowered due to dilution. No coagulation was measured to take place inside the flasks.
3. Diffusion from the pipe to the flasks, when the solenoid valves were closed, was measured to be negligible. This was checked by visual observation and by measuring the particle number density inside the flasks by means of the Coulter Counter.
4. Finally by selecting the diameter of the pipette (1/4-inch) to be larger than the pipe boundary layer and by increasing the pressure of the system so that the withdrawal velocity (500 cm/sec) was larger than the average pipe velocity (~ 180 cm/sec) we were ensured

that the sample withdrawn was representative of the conditions prevailing in the core of the fully developed turbulent pipe flow.

3.5 Particle Number Density Analysis

An excellent survey of the different ways of measuring particle or drop size distributions is given by Carver (1971), wherein seventeen particle analyzers have been listed. We decided that the Coulter Counter was the most suitable method for the present experiments. An excellent description of this method can be found in the paper by Wachtel and La Mer (1962), while an in-depth analysis of its operation is given in the paper by Colibersuch (1972).

The theory behind the operation of the Coulter Counter is quite simple. The dispersed particles suspended in 1 per cent aqueous solution of sodium chloride are forced to flow through a small aperture having an immersed electrode on each side. As each particle passes through the aperture, it replaces a volume of an electrolyte equal to its own value within the aperture, thus momentarily changing the resistance between the electrodes. This produces a voltage pulse of short duration having a magnitude proportional to the particle volume. The resulting series of pulses is electronically amplified, rated, and counted. Thus not only the total number of particles in a measured volume are counted for each sample, but their size distribution can also be measured. Apertures of different sizes can be used for different ranges of particle sizes.

In the present experiments we had to use a relatively old model (1966), model B, of the Coulter Counter supplied by the U. S. Navy.

Extensive electronic noise from electromagnetic radiation generated by other laboratory equipment was eliminated by shielding the Coulter Counter. Aperture tube sizes of 19 μm , 50 μm , 200 μm were used in the present experiments. An aperture tube can measure particles with diameters ranging from 2 per cent to 40 per cent of its size.

The 1 per cent aqueous solution of sodium chloride was twice filtered through a Millipore filter of 0.1 μm pore size (Millipore Co., Mass.) to avoid any background count.

Calibration of the Coulter Counter was done using prototype monodisperse particles supplied by the manufacturer of the equipment. It is based on the proportionality of the response to the volume of the particles. For the 19 μ tube the proportionality constant, using 0.8 μm Dow latex particles, was found to be $6.8 \times 10^{-3} (\mu\text{m})^3$ /indication of the equipment.

The actual particle size analysis of each sample was carried in a standard way. In each stage the degree of dilution was known, so that from the final measurements in the Coulter Counter, the number particle density in the pipe flow could be estimated. The Coulter Counter measures directly the cumulative particle size distribution in discrete steps. The cumulative particle size distribution gives the number of particles with volumes equal to or larger than a specified particle volume.

Finally, the maximum error in the counting of dispersed particles by the Coulter Counter was found to be ± 3 per cent deduced from numerous recordings at each indication of the equipment.

3.6 Choice of Dispersed Particles

Several types of dispersed systems were under consideration before this experimental work started. It was decided that latex particles dispersed in water were the most suitable. These latex particles are commercially available, have relatively narrow particle size distribution, and are spherical.

From preliminary estimations and experiments using the flow systems described previously, it was found that a quantity of water 200 cm^3 in volume with 10 per cent concentration in latex particles was needed for a particular run, so that a measurable degree of coagulation would take place in our system. This consumption of the latex particle dispersion made prohibitively expensive the use of uniform latex emulsions supplied by Dow Chemical or Particle Information Service. Instead we used a much more amenable acrylic latex dispersion supplied by UCAR Co. with the commercial name UCAR Latex 878.

Its average particle diameter was directly measured by taking an electronmicrograph of the dispersed particles and by analyzing the dispersion by means of the Coulter Counter. The average particle diameter was measured to be $0.59 \mu\text{m}$ with standard deviation $0.07 \mu\text{m}$. The mean particle volume defined in Equation (2-23) was estimated to be $0.15 (\mu\text{m})^3$. The density of the dispersed particles, invoked from measurements of the emulsion density, was 1.15 gm/cm^3 . The concentration in weight of the stock supplied by the manufacturer (50.8 per cent) was measured repeatedly by drying a certain quantity of the emulsion (see, e.g., Blackley (1966)).

3.7 Preparation and Destabilization of the Latex Polymer Emulsion

It is generally accepted (Van den Hul and Wanderhoff (1970)) that the surface properties of polymer lattices result from a combination of

intrinsic properties and the emulsifier imposed by the manufacturer to insure stability of the dispersion for a long time. In the present experiments the emulsion was diluted with distilled filtered water to a concentration 10 per cent in weight and was stored in the emulsion tank at least one day before an experiment was run.

After preliminary experimentation with salts and acids as destabilizers, the most effective destabilizer for the acrylic latex used in these experiments was a mixture of HCl and CaCl_2 . An aqueous solution of 1M/lt HCl and 5.6 M/lt CaCl_2 was used in all experiments. The density of this solution was measured to be 1.38 gm/cm^3 . The volumetric concentration of the above solution inside the turbulent pipe flow varied from 1 per cent to 10 per cent. The change of the physical parameters of the system due to the mixing of the destabilizer was measured prior to the analysis of the experimental results. The density of the continuous phase varied from 1 gm/cm^3 for pure water to 1.038 gm/cm^3 for the maximum concentration of the destabilizer. The viscosity of the mixture in the pipe was measured by a Cannon-Fenske viscometer in a precision temperature control viscosity bath supplied by Precision Scientific Co. (Chicago). Figure 6 depicts the relative kinematic viscosity vs. the destabilizer volume concentration of the above mixture at a typical temperature of 23° C . From this figure it is seen that the kinematic viscosity varied only slightly, namely, from 1 to $1.1 \text{ cm}^2/\text{sec}$ for the range of the destabilizer concentrations used in these experiments.

The influence of the destabilizer on the surface properties of the latex particles in thermal equilibrium was investigated by measuring

their Brownian coagulation rates for varying destabilizer concentrations and the zeta surface potential for destabilizer concentrations near the one corresponding to zero surface charge effects. These results are presented in the next chapter.

3.8 Experimental Procedure

A typical experimental run was carried out in the following way. Constant flow rate was established by means of the overflow tank shown in Figure 3. The flow rate was measured by the rotameter also shown in Figure 3.

Injection of the emulsion and the destabilizer from the respective pressurized tanks was obtained automatically by a timer through two solenoid valves. A typical injection time was 10 sec and was selected so that steady flow conditions prevailed between sampling stations one to five (see Figure 3) before a sample was withdrawn.

Samples at stations one to five were taken through solenoid valves near the end of the injection period for a typical time less than one second. The quantity sampled at each station was invoked by measuring the water displaced from each flask.

A measured quantity from each flask was next diluted in a beaker containing 120 cm^3 of an aqueous solution of 1 per cent sodium chloride. Finally these samples were used to directly measure the particle size distribution with the Coulter Counter.

Further information concerning exact dimensions of the experimental components is presented in Table I (page 78).

4. PRESENTATION AND DISCUSSION OF RESULTS

4.1 Characteristics of Turbulent Pipe Flow

Before correlating the experimental results of turbulent coagulation rate, the turbulent characteristics, as energy dissipation per unit mass, Kolmogorov time scale and Kolmogorov microscale of turbulence inside the pipe flow had to be known. Fortunately the fully developed turbulent pipe flow has been extensively investigated (Rotta (1972)). Considerable effort has been made in this work to ensure that the flow was fully developed along the test section as we have already described in the Section 3.2.

According to the classical experiments by Laufer (1954), the fully developed turbulent pipe flow is approximately isotropic up to 90 per cent of the radius from the pipe axis. In the present experiments the sampling method was designed, as it has been described in the Section 3.4, so that a sample representative mostly of the conditions prevailing in the core of the pipe was withdrawn. Hence the turbulent characteristics at the core of the pipe were used in correlating the experimental results.

The rate of turbulent energy dissipation per unit mass at the core of the pipe flow (Laufer (1954)) is

$$\epsilon = 4 \frac{u_*^3}{D_p} \quad (4-1)$$

Here u_* is the friction velocity, and D_p is the pipe diameter. The friction velocity is given by

$$u_* = U\sqrt{f/8} \quad (4-2)$$

where U is the average pipe velocity, and f is the turbulent friction coefficient for smooth pipes

$$f = \frac{0.316}{\text{Re}^{1/4}} . \quad (4-3)$$

It follows that, for a certain flow rate and pipe diameter, the Kolmogorov microscale $((\frac{v^3}{\epsilon})^{1/4})$ and the time scale $((\frac{v}{\epsilon})^{1/2})$ of turbulence at the core of the pipe can be readily estimated.

4.2 Brownian Coagulation Rate and Particle Surface Potential

Experiments to measure the Brownian coagulation rate were conducted in parallel with the turbulent coagulation experiments using the same latex dispersion. The purpose of these experiments was twofold. First, the value of the destabilizer concentration for which the dispersion becomes fully destabilized can be defined, and second, the values of Brownian coagulation rates can be compared with the turbulent coagulation rates under similar destabilizer concentrations.

Neglecting viscous interactions during particle collisions (see, e.g., Spielman (1970)), the change of particle number density with time in a Brownian coagulation process (Smoluchowski (1916)) is

$$\frac{dN}{dt} = - b N^2 . \quad (4-4)$$

The volume Brownian coagulation rate b is equal to

$$b = \frac{4kT}{3\mu} . \quad (4-5)$$

For room temperatures (20° C) and dispersions in water, the value of b is $5.4 \times 10^{-12} \text{ cm}^3/\text{sec}$.

Equation (4-4) also describes the particle number density evolution with time in partially destabilized dispersions, the coefficient on the right-hand side taking on a smaller value (Swift and Friedlander (1964)).

The particle size distributions in the Brownian coagulation experiments were measured by means of the Coulter Counter where samples taken from a beaker at specified time intervals were analyzed. The volumetric destabilizer concentration varied from 1 per cent to 10 per cent and the volume fraction of the dispersed phase from 10^{-4} to 10^{-3} .

Figures 7 and 8 show the measured experimental inverse particle number density vs. time for two different destabilizer concentrations. The associated value of the coefficient b is also given.

The ratio of the volume Brownian coagulation rate (b) for a fully destabilized dispersion to the value for a partially destabilized dispersion is called stability factor W_{Br} of the dispersion (Reerink and Overbeek (1954)). A log-log plot of the stability factor vs. the destabilizer concentration is shown in Figure 9. A linear experimental fit according to theoretical analysis (Reerink and Overbeek (1954)) and previous related experience (Ottewill and Shaw (1966)) is also drawn in this figure. The slope of this line is 1.7.

From this figure it is deduced that full destabilization of the dispersion is expected for destabilizer concentrations larger than 4.5 per cent.

Measurements of the potential, usually denoted as zeta potential, of the latex particles were attempted for destabilizer volumetric

concentrations 1 per cent to 10 per cent by the method described in Black and Smith (1962). The zeta potential was found to be very small in this range of destabilizer concentrations, approximately - 1.5 mV with an estimated error ± 30 per cent.

In Appendix B an estimate of the Brownian stability factor near the destabilizer concentration necessary for full destabilization of the dispersion is obtained.

The apparent zero surface charge, where the zeta potential is equal to zero, observed here, may be due to both an essentially chargeless surface and the ionic strength acting to swamp the surface potential (see, e.g., Ottewil and Watanabe (1960)).

4.3 Turbulent Coagulation Rate Experiments

In the present experiments the pipe flow rate varied from 5 gpm to 15 gpm, the volume fraction of the dispersed phase from 0.1 per cent to 0.5 per cent, and the volumetric destabilizer concentration from 1 per cent to 10 per cent. The particles used in the experiments described in this section had always a diameter less than the Kolmogorov microscale.

Samples were taken at each sampling station (see Figure 3) and analyzed with the Coulter Counter. The Coulter Counter measures directly the cumulative particle size distribution

$$N_v = \int_v^{\infty} n(v) dv \quad (4-6)$$

which represents the number density of particles with volume larger than the volume v .

A typical set of experimental results for the cumulative particle size distribution is presented in Figure 10. It was checked that the

volume fraction of the dispersed phase remained constant along the pipe.

In Figure 11 the experimental results of the cumulative particle size distribution are plotted in dimensionless variables, see Equations (2-25) and (2-26). From this plot it is seen that the particle size distribution remains similar to the initial particle distribution at station one. Due to the limited length of the pipe no experiments could be run to test whether the particle size distribution remains self similar for times much larger than the characteristic coagulation time.

Recent analytical studies by Pulvermacher and Ruckestein (1974) have shown that for the present collision function in Equation (2-31), there cannot exist a self-similar solution. Instead, the dimensionless particle size distribution $\psi(\xi, t)$ (see Equation (2-26)) is an explicit function of time.

Nevertheless, in the present experiments, as we mentioned previously, the particle size distribution remains approximately similar to the initial particle size distribution. This means that the polydisperseness factor $A(t)$ (see Equation (2-31)) is approximately constant. Using the curve of Figure 11, passing through the experimental results, we compute that

$$A(t) = 0.90 . \quad (4-7)$$

In Figures 12, 13, and 14 the measured total particle number density is plotted vs. distance along the pipe flow for different flow rates. Specifically the ratio of the number of particles at a sampling station

to the number of particles at the first station is the ordinate.

The abscissa is the time required for the dispersion to flow between sampling stations

$$t = \frac{x}{U} \quad . \quad (4-8)$$

Here x is the distance along the pipe from the first sampling station.

The experimental points in Figures 12, 13, 14 lie for the same degree of destabilization in a straight line in accordance with the theoretical predictions if the coagulation rate is constant (Equation (2-30)). The slope of this line, equal to the coagulation rate, increases absolutely with the destabilizer concentration.

The coagulation rate has been measured for several destabilizer concentrations and volume fractions of the dispersed phase. The dimensionless coagulation rate $\frac{\omega\tau}{\phi}$ vs. the destabilizer concentration ϕ_D is depicted in Figures 16, 17, and 18 for different flow rates. The Kolmogorov time scale $[(\nu/\epsilon)^{1/2}]$ has been estimated using Equation (4-1) and plotted in Figure 15.

Concerning the results presented in Figures 16, 17, 18, we make the following remarks:

1. For destabilizer volumetric concentrations ϕ_D larger than 5 per cent the dimensionless coagulation rate remains constant. This implies that for these concentrations the dispersion becomes fully destabilized, and the coagulation rate equals effectively to the collision rate between particles. The value ϕ_D of 5 per cent compares favorably with the value of the destabilizer concentration necessary for

full dispersion destabilization in Brownian coagulation ($\phi_D = 4.5$ per cent).

2. The value of the measured dimensionless coagulation rate for fully destabilized dispersions ($\phi_D > 5$ per cent) is

$$\frac{\omega\tau}{\phi} = 0.78 . \quad (4-9)$$

The corresponding coagulation rate for a monodisperse system with the same volume fraction should be in accordance to Equation (2-30), and using Equations (4-7) and (4-9)

$$\frac{\omega\tau}{\phi} = \frac{0.78}{0.90} = 0.86 . \quad (4-10)$$

It is seen that this value agrees very well with the theoretical value of the coagulation rate suggested by our simple kinetic model (Equation (2-14)) for a monodisperse system.

3. For partially destabilized systems, i.e., $\phi_D < 5$ per cent, a linear fit is drawn in the log-log plots of Figures 16, 17, and 18. The linear fit is justified from the form of the stability factor (see Equation (2-48)), where the characteristic energy W_0 is linearly dependent on $\ln \phi_D$ (Reerink and Overbeek (1954)). The stability factor, as in the case of Brownian coagulation, is defined as the ratio of the coagulation rate of a fully destabilized dispersion to the coagulation rate of a partially destabilized dispersion. The turbulent stability factor W_{turb} measured in these experiments is plotted in Figure 19. A linear fit is again drawn for the partially destabilized systems. It is remarkable to notice that according to the experimental results the slopes in a log-log plot

of the stability factor vs. the destabilizer concentration in a Brownian or turbulent coagulation are approximately the same. Specifically, it should be expected that for turbulent coagulation the stability factor in comparison with Brownian coagulation should be smaller due to higher collision energies. Nevertheless, it has been observed by previous investigators (Swift and Friedlander (1964) and Hahn and Stumm (1968)) that the stability factor does not essentially depend on the particle transport mode. We were not able to explain this behavior for turbulent coagulation.

Concluding the current discussion we present in Figure 20, properly plotted, experimental results by Edzwald (1972), who used two kinds of clay (kaolinite and montmorillonite). He carried out experiments in agitator tanks and measured the coagulation rate of the clay dispersions under constant turbulent agitation and varying sodium chloride concentrations. Unfortunately he did not measure the coagulation rate for fully destabilized dispersions. The turbulent stability factor in Figure 20 is the ~~inverse~~ ratio of the measured coagulation rate in a partially destabilized dispersion to the coagulation rate in a fully destabilized dispersion given by the theoretical Equation (2-14).

From experimnts by Hahn and Stumm (1970) the salt concentration for complete destabilization of montmorillonite has been found to lie between 0.44 M/lt to 0.65 M/lt NaCl. This implies that the stability factor will be constant for concentrations larger than approximately 0.55 M/lt, and this is shown by the dotted horizontal line in Figure 20. Furthermore, by extending the experimental line corresponding to partially

destabilized kaolinite dispersions until it meets the previously defined constant stability factor line, it is deduced that the destabilizer concentration for complete destabilization of the kaolinite dispersion is larger than 0.85 M/lt as it is also supported by other independent experimental results (Hahn and Stumm (1970)).

It can be found from the data of Figure 20 that the turbulent coagulation rate for a fully destabilized dispersion in agitator tanks is

$$\frac{\omega T}{\phi} = 0.19 \quad . \quad (4-11)$$

The discrepancy from the value found in Equation (4-10) may be attributed to both turbulent flow inhomogeneities in agitator tanks compared to turbulent pipe flows, and the higher degree of polydispersity of clay dispersions in contrast to the latex particles.

Finally, for fully destabilized dispersed systems we plot in Figures 21 and 22 the measured coagulation rate vs. the dispersed phase volume fraction, and the measured coagulation rate vs. the ratio of the particle size to the Kolmogorov microscale, respectively. It is seen that for the range of the variables in Figures 21 and 22, the dimensionless coagulation rate is independent of either the volume fraction of the dispersed phase or the ratio of the particle size to the Kolmogorov microscale. This agrees with the theoretical predictions (see Equation (2-14)).

5. BREAKUP OF DISPERSED PARTICLES IN ISOTROPIC TURBULENT FLOWS

Although it is doubtful that there exists an inertial subrange of turbulence in the fully developed turbulent pipe flow, we tried to run some experiments during the course of the present work using particles of size larger than the Kolmogorov microscale. Since latex particles made by Dow Chemical could not be used, because they were prohibitively expensive, we followed another course. The dispersion of latex particles provided by Union Carbide was destabilized and left to coagulate to a specified degree in the emulsion tank (see Figure 3), prior to injecting it into the pipe flow. The same procedure, as described in Chapter 3, was followed for taking samples and analyzing them by the Coulter Counter. An aperture tube of size 200 μm was used for these experiments. A high flow rate (15 gpm) was established in order to decrease the size of the Kolmogorov microscale (45 μm for the mentioned flow rate). The average particle size in the initial dispersion was measured to be 50 μm . The results did not show any variation of the total number density or particle size distribution along the pipe because simultaneously with coagulation breakup of particles was taking place. No rational analysis of the results was obtained due to the small variation of the total particle number density along the pipe in the present experiments.

Reviewing the literature we found that although the maximum particle size in the inertial subrange of turbulence is well predicted by the theories of Kolmogorov (1949) and Hinze (1955), no sound theoretical prediction of the breakup rate of particles in turbulent flows has been suggested. Knowledge of this rate could permit the evaluation of the

steady particle size distribution when both breakup and coagulation of particles are important.

An estimate of the particle breakup rate in isotropic turbulent flows is obtained in the following way. Two are the main mechanisms which could make a particle break in an isotropic turbulent flow, namely, turbulent pressure fluctuations at the ends of a particle diameter and/or forces due to the relative motion of the particle with respect to the surrounding fluid. For particles dispersed in water, turbulent pressure fluctuations dominate in general because the slip velocity of the particle is small (cf. Equation (2-7) and (2-8)).

Two distinct cases of turbulent action have to be distinguished. For particles of size larger than the Kolmogorov microscale, normal pressure fluctuations across a particle diameter dominate in comparison with shear stresses, while for particles with size less than the Kolmogorov microscale, shear stresses dominate over normal pressure fluctuations (see, e.g., Batchelor (1951)). Moreover, the resistance of the particle to deformation and breakup depends on the kind of its material. For solid particles it is shear or tensile yield stress, while for liquid particles it is surface tension. Flocs, which consist of rather loosely connected solid particles, have a solid-like behavior but with much lower values of shear or tensile strength (see Parker et al. (1972)).

A particle will break due to turbulent fluctuations across its diameter, if the instantaneous turbulent relative velocity across its diameter becomes larger than a certain velocity, defined below, necessary to break the particle.

For particles of size larger than the Kolmogorov microscale, where normal pressure fluctuations dominate, the necessary condition for breakup, based on dimensionless arguments, is expressed by the approximate relation

$$\frac{u_b}{d} \approx \left(\frac{\sigma}{\rho d^2}\right)^{1/2} \quad (5-1)$$

Here u_b is the instantaneous turbulent relative velocity across a particle diameter necessary to break a particle, and σ is the strength of the particle material to deformation.

For particles of size less than the Kolmogorov microscale, where shear stresses dominate, the necessary condition for particle breakup becomes

$$\mu \frac{u_b}{d} \approx \sigma f(\mu_d/\mu) \quad (5-2)$$

Here μ is the viscosity of continuous phase, μ_d the viscosity of particle, and f is a function depending on details of the flow (see, e.g., Taylor (1934)).

The strength of the particle material will be

$$\sigma = \text{shear or tensile strength for solid particles or flocs} \\ \text{(Parker et al. (1972))} \quad (5-3)$$

and

$$\sigma = \frac{4\gamma}{d} \text{ for liquid drops} \quad (5-4)$$

where γ is the drop interfacial tension.

For breakup to actually happen whenever the relative instantaneous velocity becomes higher than the value given by Equations (5-1) and

(5-2), the characteristic time this velocity stays higher than u_b (during which turbulent pressure forces act on the particle sufficient to break it) must be larger than the characteristic time of particle deformation which is equal to $(\frac{\sigma}{\rho d^2})^{-1/2}$ for $d > \lambda$ or $[\frac{\sigma f(u_d/\mu)}{\mu}]^{-1}$ for $d < \lambda$. (See a related discussion by Taylor (1949) for the breakup of particles in transient flows.)

The characteristic time of turbulent fluctuations across a particle diameter is equal to

$$\tau \approx \sqrt{\nu/\epsilon} \quad \text{for } d < \lambda \quad (5-5)$$

$$\tau_d \approx \frac{d}{(\epsilon d)^{1/3}} \quad \text{for } d > \lambda \quad (5-6)$$

We assume that the characteristic time of turbulent fluctuations is larger than the time characteristic of particle deformation which is generally true for particles of size either less or larger than the Kolmogorov microscale of turbulence.

We conclude that breakup of a particle will take place whenever the instantaneous turbulent relative velocity across its diameter becomes larger than the value given in Equations (5-1) and (5-2). Then the breakup rate will be equal to the frequency of crossings of the velocity u_b with positive acceleration by the statistical field of turbulent velocity differences across a particle diameter. This frequency is given by the Rice-Kac formula (see Wax (1954)), well known in statistical mathematics

$$\omega_b = \int_0^\infty p(u_b, \dot{u}) \dot{u} \, d\dot{u} \quad (5-7)$$

Here ω_b is the particle breakup rate, \dot{u} is the turbulent relative acceleration between two points at a distance of a particle diameter, and $p(u, \dot{u})$ is the joint probability density of u and \dot{u} .

We may assume that u, \dot{u} are statistically independent, which is not exactly true, but a reasonable approximation for a local description of the turbulent flow. Then Equation (5-7) can be written as

$$\omega_b = p(u_b) \int_0^{\infty} p(\dot{u}) \dot{u} d\dot{u} \quad (5-8)$$

Or finally the breakup rate will be equal to

$$\omega_b \approx 2(\overline{\dot{u}^2})^{1/2} p(u_b) \quad (5-9)$$

Here $(\overline{\dot{u}^2})^{1/2}$ is the root mean square turbulent acceleration difference across a particle diameter, and the factor 2 is associated with an unskewed velocity probability density. The turbulent acceleration is approximately (Levich (1962)) equal to

$$(\overline{\dot{u}^2})^{1/2} \approx \frac{u_r}{\tau} = \frac{\epsilon d}{\nu} \quad \text{for } d < \lambda \quad (5-10)$$

$$(\overline{\dot{u}^2})^{1/2} \approx \frac{u_r}{\tau_d} = \frac{(\epsilon d)^{2/3}}{d} \quad \text{for } d > \lambda \quad (5-11)$$

We may approximate (see also discussion after Equation (2-13) in Section 2.2) the relative velocity probability density $p(u)$ by a Gaussian probability density with a cutoff velocity u_c both in the laminar subrange and the inertial subrange of isotropic turbulence (see Townsend (1947) and Van Atta and Park (1972)). It follows that the breakup rate (Equation (5-9)) will take the form

$$\omega_b \approx \frac{B}{\tau_b} \left[\exp \left(-\frac{u_b^2}{2u_r^2} \right) - \exp \left(-\frac{u_c^2}{2u_r^2} \right) \right] . \quad (5-12)$$

Here B is a proportionality breakup constant of order one, u_b is given from Equation (5-1) or (5-2), and the breakup characteristic time will be

$$\tau_b = \tau = \sqrt{\nu/\epsilon} \quad \text{for } d < \lambda \quad (5-13)$$

$$\tau_b = \tau_d = \frac{d}{(\epsilon d)^{1/3}} \quad \text{for } d > \lambda . \quad (5-14)$$

Finally, u_r is the root mean square velocity difference across a particle diameter equal to (Rotta (1972))

$$u_r \approx \sqrt{\epsilon/\nu} d \quad \text{for } d < \lambda \quad (5-15)$$

$$u_r \approx (\epsilon d)^{1/3} \quad \text{for } d > \lambda . \quad (5-16)$$

Equation (5-12) is quite general, and it can be applied to either solid or liquid particles dispersed in water with sizes less or larger than the Kolmogorov microscale.

We can now write down the kinetic equation for the evolution of particle size distribution with time including breakup effects. Assuming only binary collisions and that each particle breaks into two particles of equal volume, we get

$$\begin{aligned} \frac{dn(v,t)}{dt} = & 1/2 \int_0^v n(v',t) n(v-v',t) \omega(v', v-v') dv' \\ & - \int_0^\infty n(v',t) n(v,t) \omega(v,v') dv' + 4\omega_b(2v) n(2v,t) - \omega_b(v) n(v,t) . \end{aligned} \quad (5-17)$$

Here $\omega_b(v)$ is the breakup rate of a particle with volume v given by Equation (5-12).

It is not the scope of the present work to analyze in detail the consequences of Equation (5-17). Besides there are not experimental data for the determination of the proportionality constants in the expression for the breakup rate in Equation (5-12). Indications that Equation (5-12) may be correct have been presented in a recent paper by Delichatsios and Probstein (1973), where Equation (5-12) and (5-17) were used to explain the experimental results for the steady drop size of dense oil in water emulsions inside agitator tanks.

In Table II (page 79) the conditions of maximum particle size are listed for dilute dispersions where coagulation is negligible. In this case the maximum particle size is determined from the condition that ω_b must be equal to zero. Then Equation (5-12) gives

$$\frac{u_b^2}{u_r^2} = \left(\frac{u_c}{u_r} \right)^2 = \text{constant} . \quad (5-18)$$

6. SCALING LAWS AND APPLICATIONS IN WASTEWATER TREATMENT SYSTEMS

6.1 Scaling Laws

The separation of dispersed solid particles from wastewaters by coagulation, followed by sedimentation or filtration is one of the methods frequently used in wastewater treatment systems. Destabilization of the particle dispersion is a necessary step before coagulation begins. Optimum dosages of coagulant and/or coagulant aids have been established for different dispersions depending on the physicochemical properties of the dispersed particles (Cohen and Hannah (1971)).

The efficiency of the separation, after the dispersion is chemically destabilized, depends on the interaction and relative importance of coagulation, breakup, and settling of the particles by gravitational action.

Thus it becomes apparent that a detailed knowledge of the effects of coagulation, breakup, and sedimentation in a separation system, coupled with the knowledge of the physicochemical properties of the system, will be valuable for a rational design of a wastewater treatment plant.

We can readily plot the regimes in which coagulation, breakup, or sedimentation dominate based on the knowledge gained in this work. We assume, as it usually happens in practice, that turbulent flow transports the particles, and it can be considered at least locally isotropic.

The results are appropriately shown in Figure 23 where the different regimes have been marked. Brief explanation about each regime in Figure 23 is given below.

Line A, which serves as a limit of turbulent coagulation dominance over Brownian coagulation, is drawn using Equation (2-38). Line B gives the Kolmogorov microscale of turbulence ($\lambda = \frac{v^3}{\epsilon}^{1/4}$).

Line C for drop breakup can be derived from the results listed in Table II. The equation used to draw line C is

$$\frac{\rho \epsilon^{2/3} d^{5/3}}{\gamma} = 0.075 \quad . \quad (6-1)$$

Here the constant (0.075) has been deduced from the experimental results by Sprow (1967). The drop surface tension in Equation (6-1) has been taken equal to 40 dyn/cm.

Line E for floc breakup has been constructed using again the results from Table II. For flocs larger than the Kolmogorov microscale the maximum particle size will be

$$d = \frac{c}{\epsilon} \quad (6-2)$$

where the constant c is proportional to $(\frac{\sigma}{\rho})^{3/2}$. This constant has been determined equal to $0.71 \text{ cm}^3/\text{sec}^3$ from experiments on ferric floc breakup presented in Parker et al. (1972). For flocs less than the Kolmogorov microscale, the delimiting line is given by (see Table II)

$$\epsilon = \text{const} \quad . \quad (6-3)$$

The constant in the last equation has been determined from the requirement that for floc sizes of the order of the microscale of turbulence, Equations (6-2) and (6-3) must give the same value of the ferric floc size (see Figure 23).

Gravitational effects, depicted by line D in Figure 23, will be important, when the settling velocity of the particle is of the same order of magnitude as the root mean square velocity of the turbulent flow (see Equations (2-1) and (2-2). In drawing line D we have taken

$$\frac{(\rho_p - \rho)}{\rho} = 0.2, \rho = 1 \text{ gm/cm}^3, \nu = 10^{-2} \text{ cm}^2/\text{sec}, \text{ and } L = 10 \text{ cm or } L = 1 \text{ cm.}$$

Figure 23 may be used in quite different flow situations as long as the rate of energy dissipation per unit mass ϵ and the macroscale of turbulence L are properly determined. In pipe flows the energy dissipation is given by Equation (4-1), and the macroscale of turbulence is equal to (see, e.g., Powe and Townes (1972))

$$L = 0.05 D . \tag{6-4}$$

In agitator tanks the rate of energy dissipation and the macroscale of turbulence have been lately measured by Lattke (1971). In this case the energy dissipation may be approximated by

$$\epsilon = \frac{P}{\rho V_T} . \tag{6-5}$$

Here P is the power input by the impeller, ρ the density of the dispersion, and V_T the tank volume. The macroscale of turbulence is typically equal to

$$L = 0.04 D_T \tag{6-6}$$

where D_T is the diameter of the tank.

6.2 A New Approach to Wastewater Treatment

By intelligently utilizing the information gained from Figure 23, we propose in what follows a new method and apparatus for wastewater treatment in a small community, for example, a ship (Probstein and Delichatsios (1974)).

A block diagram of this system is shown in Figure 24. The general characteristics of this method are described below.

Coagulation of micron or submicron particles, denoted as primary particles, takes place to the required degree inside a turbulent pipe flow. Coagulation by turbulent action follows chemical destabilization and is completed to the required degree, prior to discharging the dispersion into the sedimentation tank. In order to increase the efficiency of the coagulation, a controlled quantity of flocculated particles is recirculated from the sedimentation tank and injected into the turbulent pipe flow where coagulation takes place. The pipe diameter is selected in such a way that the recirculated flocs do not break, and no deposition of flocculating particles is probable inside this pipe.

The rate of removal of the primary particles in the proposed apparatus is invoked from the theoretical and experimental investigation of the present thesis (Chapters 2, 3, 4). The principal mode of removal of these particles in the pipe flow is by coagulating with the floc recirculated from the sedimentation tank. In wastewater treatment systems the size of the primary particles and flocs is in general less than the Kolmogorov microscale. Thus the rate of coagulation of the primary particles of size d_1 with the flocs, assuming the respective dispersions to be monodisperse, can be expressed by the following relation

$$\omega_{1F} \approx \pi \left(\frac{d_1 + d_F}{2} \right)^2 u_r \cdot N_F \quad (6-7)$$

Here d_F is the floc diameter, N_F is the number density of flocs, and the relative velocity u_r is equal (Equation (2-20) to

$$u_r = \sqrt{1/15} \sqrt{\epsilon/v} \left(\frac{d_1 + d_F}{2} \right) \quad (6-8)$$

Since the size of the primary particles ($\sim 1 \mu\text{m}$) is much less than the size of recirculated floc ($\sim 90 \mu\text{m}$), Equation (6-7) may be written using Equation (6-8) as

$$\frac{\omega_{1F}^T}{\phi_F} = 0.2 \quad . \quad (6-9)$$

Here ϕ_F is the volume fraction of the recirculated floc

$$\phi_F = \pi/6 d_F^3 N_F \quad . \quad (6-10)$$

The rate of removal of primary particles will be given by

$$\frac{dN_1}{dt} = - \omega_{1F} N_1 \quad (6-11)$$

where N_1 is the number density of the primary particles.

The basic advantage of the present method is that the space requirements for such a wastewater system, for example, in a ship, are reduced to at least one order of magnitude compared with other conventional systems, as it is shown in Appendix C. Moreover, it should be pointed out that the present system combined with compact carbon reactors for the removal of organic wastes can be an advantageous system for wastewater treatment (see, e.g., the paper by Weber (1972)).

7. CONCLUSIONS AND RECOMMENDATIONS

The main results of this thesis are listed briefly below.

1. A simple binary collision kinetic model was successful in predicting the coagulation rate of destabilized monodisperse colloidal particles in isotropic turbulent flows.
2. The same model applied to polydisperse systems showed that the effective coagulation rate in a polydisperse system is reduced compared to the coagulation rate of a monodisperse system with the same dispersed phase volume fraction.
3. An estimate of the retarded coagulation rate due to interparticle potential repulsion was obtained for dispersed particles of sizes less than the Kolmogorov microscale.
4. Experiments carried out in fully developed turbulent pipe flows determined the important parameters which control the coagulation process. Flow rate, destabilizer concentration, and volume fraction of the dispersed phase were the working variables. The particle sizes were less than the Kolmogorov microscale.
5. The experiments showed that the coagulation stability factor for partially destabilized dispersions in turbulent flows is approximately equal to the coagulation stability factor in Brownian motion in consistency with previous observations (Hahn and Stumm (1968)), but a thorough understanding of the reasons remains to be obtained.
6. Experiments with particle sizes larger than the Kolmogorov microscale did not give gainful results since breakup of particles was simultaneously taking place.

7. A new model for the particle breakup rate in isotropic turbulence was developed, and the maximum particle size has been obtained for solid or liquid particles of various sizes in dilute dispersions.
8. Scaling laws have been developed for the relative importance of coagulation, breakup, and sedimentation of particles in a wastewater treatment system employing coagulation and sedimentation.
9. A new wastewater treatment method, considerably reducing the space requirements, has been proposed employing turbulent pipe flow coagulations and floc recirculation from the sedimentation tank.

Recommendations for further research related to the present work are given below.

1. Direct measurements of the breakup rate of particles in turbulent flows could help verify the theoretical model suggested here.
2. Using the result for breakup rate, experiments to measure the coagulation rate in turbulent flows for particle sizes larger than the Kolmogorov microscale could be intelligently interpreted and analyzed.
3. A theoretical and experimental analysis of the coagulation of particles in turbulent shear flows would be valuable.
4. More work should be conducted to properly characterize the "floc strength."

APPENDIX A

Limits of the Polydisperseness Coefficient A(t)

In a monodisperse system the dimensionless particle size distribution defined in Equation (2-26) is a delta function centered at 1. It follows directly from Equation (2-31) that for a monodisperse system at the onset of coagulation, the coefficient $A(t) = 1$.

In a system consisting of two monodisperse systems with particle volume fractions, diameters and number densities ϕ_1, d_1, n_1 and ϕ_2, d_2, n_2 , respectively, the evolution of the total particle number density with time at the onset of coagulation is given by

$$\frac{d(n_1 + n_2)}{dt} = -\frac{1}{2} \omega_{11} n_1^2 - \omega_{12} n_1 n_2 - \frac{1}{2} \omega_{22} n_2^2. \quad (A-1)$$

Here the symmetric tensor ω_{ij} ($i, j = 1, 2$) represents the volume swept per unit time by particles with diameters d_i and d_j during collision and can be found from Equation (2-19). For particle sizes less than the Kolmogorov microscale

$$\omega_{ij} = a \left(\frac{d_i + d_j}{2} \right)^3 \quad (A-2)$$

where the proportionality coefficient

$$a = \pi \sqrt{\frac{1}{15}} \left(\frac{\epsilon}{\nu} \right)^{1/2}. \quad (A-3)$$

Then Equation (A-1) can be rewritten in the following form

$$\frac{1}{(n_1 + n_2)} \frac{d(n_1 + n_2)}{dt} = -\omega \frac{4(n_1^2 d_1^3 + n_2^2 d_2^3) + (d_1 + d_2)^3 n_1 n_2}{4(n_1 + n_2)(n_1 d_1^3 + n_2 d_2^3)} \quad (A-4)$$

wherein Equations (A-2) and (A-3) have been used, and ω is the coagulation rate of a nonodisperse system of volume fraction $(\phi_1 + \phi_2)$ (cf. Equation (2-30)).

It follows that the coefficient $A(t=0)$ (cf. Equation (2-30) at the onset of coagulation) will be equal to

$$A(t = 0) = \frac{4(n_1^2 d_1^3 + n_2^2 d_2^3) + (d_1 + d_2)^3 n_1 n_2}{4(n_1 + n_2)(n_1 d_1^3 + n_2 d_2^3)} . \quad (A-5)$$

After some rearrangements it is found that

$$A(t = 0) = 1 - \frac{3}{4} \frac{(d_1 - d_2)^2 (d_1 + d_2) n_1 n_2}{(n_1 + n_2)(n_1 d_1^3 + n_2 d_2^3)} . \quad (A-6)$$

For the special case of two widely differing volume fractions ($\phi_1 \ll \phi_2$) and widely differing number densities in the inverse order ($n_1 \gg n_2$)

$$1 \ll \frac{n_1}{n_2} \ll \left(\frac{d_2}{d_1}\right)^3 , \quad (A-7)$$

and the value of the coefficient $A(t)$ becomes

$$A(t = 0) = 0.25 . \quad (A-8)$$

APPENDIX B

The Stability Factor in Brownian Motion Coagulation

The general form of the Brownian stability factor is given by the relation (Overbeek (1952))

$$W_{Br} = d \cdot \int_d^\infty \frac{1}{r^2} \exp \left(\int_\infty^r \frac{1}{kT} \frac{dW(r)}{dr} dr \right) dr . \quad (B-1)$$

In this equation $W(r)$ is the interparticle potential energy as a function of the distance r between the center of the particles. An estimate of the Brownian stability factor is given in the following analysis.

The interparticle potential energy can be modeled as a potential square barrier of characteristic intensity W_0 , typically equal to the maximum interparticle potential energy, acting over a distance λ_D , of the order of the Debye length (Overbeek (1952)), from the particle surface. Then using the relations

$$\frac{dW(r)}{dr} = 0 \quad \text{for } r > d + \lambda_D = r_0 \quad (B-2)$$

$$\int_\infty^r \frac{dW(r)}{dr} dr = W_0 \quad \text{for } r < d + \lambda_D = r_0 , \quad (B-3)$$

the stability factor from Equation (B-1) takes the form

$$W_{Br} = \frac{\lambda_D}{r_0} \exp\left(\frac{W_0}{kT}\right) + \frac{d}{r_0} . \quad (B-4)$$

It should be noticed that Overbeek (1952) suggested an approximate form of the stability factor

$$W_{Br} = \frac{\lambda_D}{d} \exp\left(\frac{W_0}{kT}\right) . \quad (B-5)$$

This approximate relation has been frequently quoted in the literature by previous investigators (see, e.g., Hahn and Stumm (1970) and Edzwald (1970)). Apparently the approximation given by Equation (B-5) will be correct, by comparison to Equation (B-4), only when $\frac{W_o}{kT} \gg 1$, namely, for large interparticle potential energies.

Another important result derived from Equation (B-4) is presented below for interparticle potential energies small in comparison with the thermal energy kT . In this case Equation (B-4) will become

$$W_{Br} = 1 + \frac{\lambda_D}{r_o} \frac{W_o}{kT} \quad (B-6)$$

by expanding the exponential expression in Equation (B-4) in Taylor series. Taking the logarithm on both sides of Equation (B-6), we get

$$\ln W_{Br} \approx \frac{\lambda_D}{r_o} \frac{W_o}{kT} \quad (B-7)$$

The value of the characteristic (maximum) potential energy W_o has been estimated by Reerink and Overbeek (1954)

$$W_o = \frac{H}{24kT} \frac{d}{s} \left(\frac{\lambda_D}{s} - 1 \right) \quad (B-8)$$

where s corresponds to the distance from the particle surface where the potential is maximum, and H is the Hamaker constant associated with Van der Waal's attraction.

For coagulation conditions near the value where $W_o = 0$, we may consider $\frac{\lambda_D}{s} \approx 1$ and $s = \text{constant}$ (see Reerink and Overbeek (1954)).

Using Equation (B-8) and after some rearrangements (see also Reerink and Overbeek (1954)), we finally find that

$$\ln W_{Br} \approx - \frac{H}{48kT} \ln \phi_D + C \quad (B-9)$$

where C is a constant independent essentially of the destabilizer concentration. In deriving Equation (B-9) we have taken approximately $r_o \approx d$ and used the relation $\lambda_D \propto \phi_D^{-1/2}$.

It is seen from Equation (B-9) that

$$\frac{d(\ln W_{Br})}{d(\ln \phi_D)} = - \frac{H}{48kT} . \quad (B-10)$$

For a typical value of Hamaker constant 10^{-12} ergs and at normal room temperature 20°C , the slope in Equation (B-10) takes on the value

$$\frac{d(\ln W_{Br})}{d(\ln \phi_D)} = - 0.52 . \quad (B-11)$$

This value compares favorably with the experimental value 1.7 (see Figure 9) if account is taken of the ambiguity associated with the definition of the Hamaker constant (Reerink and Overbeek (1954)).

APPENDIX C

Shipboard Wastewater Treatment

For a cargo or Navy ship with population two hundred persons and average sewage flow for U.S.A. standards 80 gal/person day (Imhoff et al. (1971)), the steady sewage flow rate is approximately 12 gpm. The concentration of solids for dry weather conditions is 480 ppm (Imhoff et al. (1971)). The maximum content in suspended solids of the treated water required by EPA is 150 ppm. Assuming the particle size distribution not too broad, the required reduction in total particle number density to the initial value should be approximately 4.

The volume fraction of the recirculated flocs inside the pipe, where coagulation takes place is designed to be 3 per cent. Thus the flow rate in the floc recirculation system is calculated to be 5 gpm for a 10 per cent in volume fraction floc dispersion with floc size approximately 90 μm . The rate of turbulent energy dissipation per unit mass in the core of the pipe is selected to be near the maximum allowed for a typical ferric floc, i.e., 60 ergs/gm \cdot sec (see Figure 23), so that deposition or breakup of particles or flocs is negligible.

From the required flow rate of 17 gpm in the main pipe and using Equations (4-1), (4-2), and (4-3), the average pipe velocity and the pipe diameter are found to be

$$U = 76 \text{ cm/sec}$$

$$D_p = 4 \text{ cm} \tag{C-1}$$

The coagulation rate of the primary particles with the flocs will then be (from Equation (6-9))

$$\omega_{1F} = 0.5 \text{ sec}^{-1} . \quad (\text{C-2})$$

Using Equation (6-11) and Equation (C-2) the time required for coagulation in the present system (i.e., reduction of the primary particle number density by a factor of 4) is found to be

$$t = 3 \text{ sec} , \quad (\text{C-3})$$

and the length of the pipe

$$l = 220 \text{ cm} . \quad (\text{C-4})$$

The size of the sedimentation tank is now determined by the size of the flocs on which the primary particles have stuck and by the flow rate of discharged sewage. Assuming $\frac{\rho_p - \rho}{\rho} = 0.2$ and the minimum size of the flocs $80 \mu\text{m}$, the settling velocity (Equation (2-1)) will be

$$u_s = 0.07 \text{ cm/sec} . \quad (\text{C-5})$$

For an effective sedimentation tank height of 50 cm, the required residence time will be 12 min. and the tank volume 28 ft^3 .

The diameter of the pipe used for floc recirculation from the sedimentation tank is determined equal to 2.7 cm for a flow rate 5 gpm. The corresponding turbulent energy dissipation rate is 70 ergs/sec gm. Thus the corresponding stable floc size in this pipe according to Figure 23 is less than the maximum floc size corresponding to the operating conditions inside the pipe where coagulation takes place.

The total volume of the present system will be approximately 30 ft^3 , almost more than one order of magnitude less than the volume of comparable conventional systems in use (Sanders (1972)). Another important

advantage of the present system is that the coagulation tank of conventional systems is eliminated, and instead existing pipes can be used as effective flocculators.

REFERENCES

- Batchelor, G. K., "Pressure Fluctuations in Isotropic Turbulence,"
Proc. Cambridge Phil. Soc. 47, 359 (1951).
- Batchelor, G. K., The Theory of Homogeneous Turbulence, p. 106, Cambridge Univ. Press, Cambridge, England (1960).
- Batchelor, G. K. and A. A. Townsend, "Turbulent Diffusion," in Surveys in Mechanics in Commemoration of the 70th Birthday of G. I. Taylor p. 352, Cambridge Univ. Press, Cambridge, England (1956).
- Batchelor, G. K., "Sedimentation in a Dilute Dispersion of Spheres,"
J.F.M. 52, 245 (1972).
- Birkner, B. F. and J. J. Morgan, "Polymer Flocculation Kinetics of Dilute Colloidal Suspensions," J. AWWA 60, 179 (1968).
- Black, A. P. and A. L. Smith, "Determination of the Mobility of Colloidal Particles by Microelectrophoresis," J. AWWA 54, 926 (1962).
- Blackley, D. C., High Polymer Lattices, MacLaren & Sons Ltd., London (1966).
- Brodkey, R. S., Mixing Theory and Practice, Academic Press, N. Y. (1966).
- Camp, T. R. and P. C. Stein, "Velocity Gradients and Internal Work in Fluid Motion," Journal of the Boston Society of Civil Engineers 30, 219 (1943).
- Carver, L. D., "Particle Size Analysis," Industrial Research, August (1971).
- Cohen, J. M. and S. A. Hannah, "Coagulation and Flocculation," in Water Quality and Treatment, p. 66, McGraw-Hill, N. Y. (1971).
- Colibersuch, D. C., "Observation of Aspherical Particle Rotation in Poiseuille Flow via the Resistance Pulse Technique. I. Application to Human Electrolytes," General Electric Technical Information Series (1972).

- Delichatsios, M. A. and R. F. Probstein, "The Effects of Holdup on Equilibrium Drop Sizes in an Agitated Tank," M.I.T. Fluid Mechanics Lab. Publ. No. 73-8 (1973).
- Edzwald, J. K., "Coagulation in Estuaries," Sea Grant Publication VNC-SG-72-06, University of North Carolina (1972).
- Fuchs, N., "Über die Stabilität und Aufladung der Aerosole," Z. Physik 89, 736 (1934).
- Hahn, H. H. and W. Stumm, "Kinetics of Coagulation with Hydrolyzed Al(III), The Rate-Determining Step," J. of Colloid and Interface Science 28, 134 (1968).
- Hahn, H. H. and W. Stumm, "The Role of Coagulation in Natural Waters," American Journal of Science 268, 354 (1970).
- Hartung, K. H. and J. W. Hiby, "Beschleunigung der turbulenten Mischung in Röhren," Chemie-Ing-Techn. 44, 1051 (1972).
- Hinze, J. O., "Fundamentals of the Hydrodynamic Mechanism of Splitting in Dispersion Processes," AIChE J. 1, 289 (1955).
- Imhoff, K., W. J. Muller, and D. K. B. Thistlethwayte, Disposal of Sewage and other Water-borne Wastes, Ann Arbor Science, Ann Arbor (1971).
- Kolmogorov, A. M., "On the Breaking of Drops in Turbulent Flow," (in Russian), Dokl. Akad. Nauk. S.S.S.R. 66, 825 (1949).
- Laufer, J., "The Structure of Turbulence in Fully Developed Pipe Flow," NACA Rept. No. 1174 (1954).
- Lattke, H., "Untersuchung über Homogenisieren and über Turbulenz in Rührmaschinen," Chem. Techn. 23, 231 (1971).

- Levich, V. G., Physicochemical Hydrodynamics, p. 213, Prentice Hall, Englewood Cliffs, N. J. (1962).
- Mlynek, Y. and W. Resnick, "Drop Sizes in an Agitated Liquid-Liquid System," AIChE J. 18, 122 (1972).
- Ottewill, R. H. and J. N. Shaw, "Stability of Monodisperse Polyesterene Dispersions of Various Sizes," Disc. Faraday Soc. 42, 153 (1966).
- Ottewill, R. H. and A. Watanabe, "Studies on the Mechanism of Coagulation," Kolloid Zeitschrift 173, 1, 8 (1950).
- Overbeek, J. Th. G., "Kinetics of Flocculation" in Colloid Science, Ed. H. H. Kruyt, p. 278, Elsevier Publishing Company, Amsterdam (1952).
- Owen, P. R., "Pneumatic Transport," JFM 39, 407 (1969).
- Parker, S. D., et al., "Floc Breakup in Turbulent Flocculation Processes," J. of the San. Engin. Div. Proc. ASCE SA1 98, 79 (1972).
- Powe, R. E. and H. W. Townes, "Turbulence Structure for Fully Developed Flow in Rough Pipes," ASME Paper 72WA/Fe-14 (1972).
- Probstein, R. F. and M. A. Delichatsios, "Method and Apparatus for Continuous Flow Flocculation and Clarification," U. S. Patent pending (1974).
- Pulvemacher, B. and E. Ruckenstein, "Similarity Solutions of Population Balances," J. of Colloid and Interface Sci. 46, 428 (1974).
- Reerink, H. and J. Th. G. Overbeek, "The Rate of Coagulation as a Measure of the Stability of Silver Iodide Sols," Disc. Faraday Soc. 18, 74 (1954).
- Roberts, P. H., "Analytical Theory of Turbulent Diffusion," JFM 11, 257 (1961).

- Rotta, J. C., Turbulente Strömungen, p. 93, B. G. Teubner, Stuttgart (1972).
- Sanders, G. A. et al., Shipboard Control of Wastes in Immediate Cost-Effective Abatement of Water Pollution from Navy Ships, p. 15, Naval Postgraduate School, Monterey, California (1972).
- Saffman, P. G. and J. S. Turner, "On the Collision of Drops in Turbulent Clouds," JFM 1, 16 (1956).
- Schlichting, H., Boundary-Layer Theory, p. 562, McGraw-Hill Co., N. Y. (1968).
- Smoluchowski, M., "Drei Vorträge über Diffusion, Brownsche Molekular Bewegung and Koagulation von Kolloidteilchen," Physik. Z. 17, 557 (1916).
- Smoluchowski, M., "Versuch einer mathematischen Theorie der Koagulations-Kinetik Kolloider Lösungen," Zeitschrift für physikalische Chemie 92, 129 (1917).
- Spielman, L. A., "Viscous Interaction in Brownian Coagulation," J. of Colloid and Interface Science 33, 562 (1970).
- Sprow, F. B., "Distribution of Drop Sizes Produced in Turbulent Liquid-Liquid Dispersions," Chem. Eng. Sci. 22, 435 (1967).
- Swift, D. L. and S. K. Friedlander, "The Coagulation of Hydrosols by Brownian Motion and Laminar Shear Flow," J. of Coll. Science 19, 621 (1964).
- Taylor, G. I., "The Shape and Acceleration of a Drop in a High Speed Air Stream" (1949), in The Scientific Papers of Sir Geoffrey Ingram Taylor, G. K. Batchelor (ed.) Vol. III, p. 457, Cambridge Univ. Press, Cambridge (1963).

- Taylor, G. I., "The Formation of Emulsions in Definable Fields of Flow," Proc. Roy. Soc. London A146, 501 (1934).
- Tempel, Den Van M., "Stability of Oil in Water Emulsions II," Rec. Trav. Chim. 72, 433 (1953).
- Townsend, A. A., "The Measurement of Double and Triple Correlation Derivatives in Isotropic Turbulence," Proc. Cambr. Phil. Soc. 43, 560 (1947).
- Van Atta, C. and J. Park, "Statistical Self-Similarity and Inertial Sub-range Turbulence," in Statistical Models and Turbulence, M. Rosenblatt and C. Van Atta (eds.), p. 402, Springer-Verlag, Berlin, Heidelberg, New York (1972).
- Van den Hul, H. J. and J. W. Vanderhoff, "Clean Monodisperse Latexes as Model Colloids," Am. Chem. Soc. Symp. on Polymer Colloids, Fitch, R. M., ed., Plenum Press, N. Y. (1971).
- Verwey, E. J. W. and J. Th. G. Overbeek, Theory of the Stability of Lyophobic Colloids, Elsevier Publ. Co., N. Y. (1948).
- Wachtel, E. R. and V. K. La Mer, "The Preparation and Size of some Monodisperse Emulsions," J. Colloid Sci. 17, 531 (1962).
- Weber, W. J., Jr., Physicochemical Processes for Water Quality Control, Wiley Interscience, N. Y. (1972).
- Weber, W. J., Jr., "Physicochemical Systems" in Progress in Water Technology, eds. Cecil, L. K. and W. W. Eckenfelder, Pergamon Press, N. Y. (1972).

TABLE I

Characteristics of the Experimental System

1. Flow System

Overflow Tank: Cylindrical steel tank with plastic inside coating
Dimensions: 76 cm in diameter, 90 cm in height
Filters: Fulflo Honeycomb filters
Rotameter: Precision Rotameter with range from 2 to 17 gpm
and accuracy ± 1 per cent of the maximum flow
rate (Fisher and Parker Co.)
Emulsion Tank: Cylindrical plexiglas tank, 8 lt in volume
Destabilizer
Tank: Same as above
Test Section: Distances between sampling stations
1-2 94 cm ± 0.5 cm
2-3 125 cm ± 0.5 cm
3-4 113 cm ± 0.5 cm
4-5 124 cm ± 0.5 cm

2. Fluid Properties

Emulsion: UCAR acrylic latex 878, with average size 0.59 μm
Destabilizer: Aqueous solution of 1 M/lt HCl and 5.6 M/lt CaCl_2
Mixture Density in Pipe: 1 to 1.04 gm/cm^3
Mixture Kinematic Viscosity in Pipe: 1 to 1.1 cm^2/sec

3. Flow Conditions

Flow Rate 5 to 15 gpm
Reynolds Number: 17,000 to 51,000
Destabilizer Concentration in Pipe: 1% to 10% in volume
Emulsion Volume Fraction in Pipe: 10^{-3} to 5.10^{-3}

TABLE II

Maximum Breakup Particle Diameter

<u>Particle Size</u>	<u>Drops</u>	<u>Flocs</u>
$d < \lambda$	$\frac{\gamma f(\mu_d/\mu)}{\mu \sqrt{\epsilon/\nu} d} = \text{const} \quad (1)$	$\frac{\sigma f(\mu_d/\mu)}{\mu \sqrt{\epsilon/\nu}} = \text{const}$
$d > \lambda$	$\frac{\gamma}{\rho \epsilon^{2/3} d^{5/3}} = \text{const} \quad (2)$	$\frac{(\sigma/\rho)^{3/2}}{\epsilon d} = \text{const} \quad (3)$

(1) see also Sprow (1967)

(2) see also Mlynek and Resnick (1972)

(3) see also Parker et al. (1972)

FIGURE TITLES

- Fig. 1 Mean square relative velocity between two points in isotropic turbulence as a function of the ratio of the distance between the points to the Kolmogorov microscale.
- Fig. 2 Theoretical reduced coagulation rate between particles in isotropic turbulent flows as a function of the ratio of the particle size to the Kolmogorov microscale.
- Fig. 3 Experimental setup.
- Fig. 4 Destabilizer injection port.
- Fig. 5 Typical sampling station.
- Fig. 6 Kinematic viscosity of the continuous phase vs. the volumetric destabilizer concentration.
- Fig. 7 Inverse particle number density vs. time from the beginning of the Brownian coagulation ($\phi_D = 2.2\%$).
- Fig. 8 Inverse particle number density vs. time from the beginning of the Brownian coagulation ($\phi_D = 4.5\%$).
- Fig. 9 Stability factor as a function of destabilizer concentration in Brownian coagulation.
- Fig. 10 Cumulative particle size distribution at different sampling stations along the pipe.
- Fig. 11 Cumulative particle size distribution at different sampling stations along the pipe in reduced similarity variables.
- Fig. 12 Particle number density relative to value at first station as a function of distance along the pipe measured in time for dispersion to flow to sampling station ($Q = 5$ gpm).
- Fig. 13 Particle number density relative to value at first station as a function of distance along the pipe measured in time for dispersion to flow to sampling station ($Q = 10$ gpm).
- Fig. 14 Particle number density relative to value at first station as a function of distance along the pipe measured in time for dispersion to flow to sampling station ($Q = 15$ gpm).
- Fig. 15 Kolmogorov time scale vs. Reynolds number in the core of turbulent pipe flows.

- Fig. 16 Measured coagulation rate vs. destabilizer concentration (Q = 5 gpm).
- Fig. 17 Measured coagulation rate vs. destabilizer concentration (Q = 10 gpm).
- Fig. 18 Measured coagulation rate vs. destabilizer concentration (Q = 15 gpm).
- Fig. 19 Stability factor as a function of the destabilizer concentration in turbulent pipe flow coagulation.
- Fig. 20 Stability factor vs. destabilizer concentration in turbulent flows inside agitator tanks .
- Fig. 21 Measured coagulation rate vs. the volume fraction of the dispersed particles in fully destabilized systems .
- Fig. 22 Measured coagulation rate vs. the ratio of the particle size to the Kolmogorov microscale in fully destabilized systems.
- Fig. 23 Particle size vs. the rate of turbulent energy dissipation per unit mass in wastewater treatment systems employing coagulation and sedimentation .
- Fig. 24 A new approach to wastewater treatment employing turbulent pipe flow coagulation .

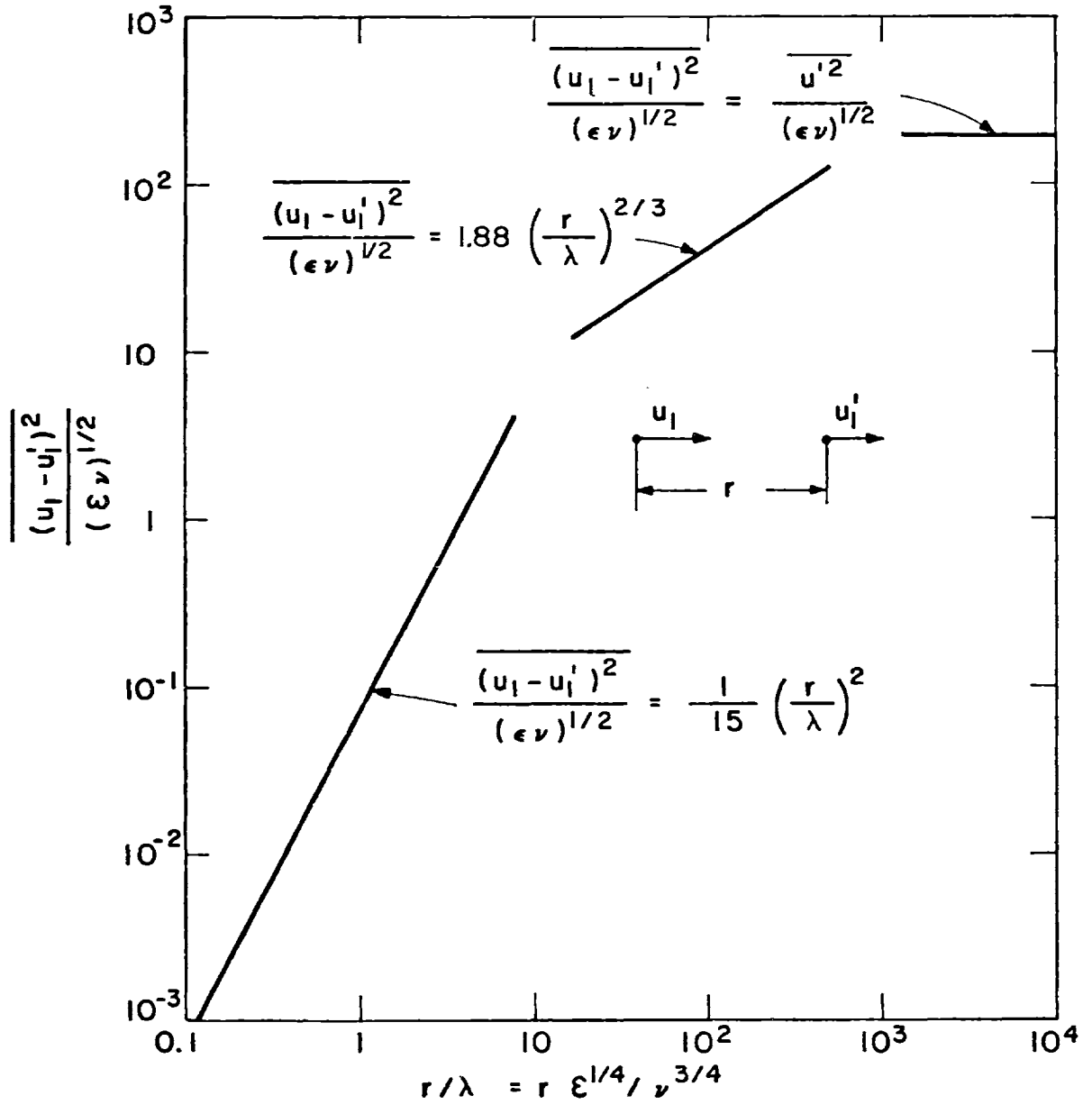


Fig. 1 Mean square relative velocity between two points in isotropic turbulence as a function of the ratio of the distance between the points to the Kolmogorov microscale.

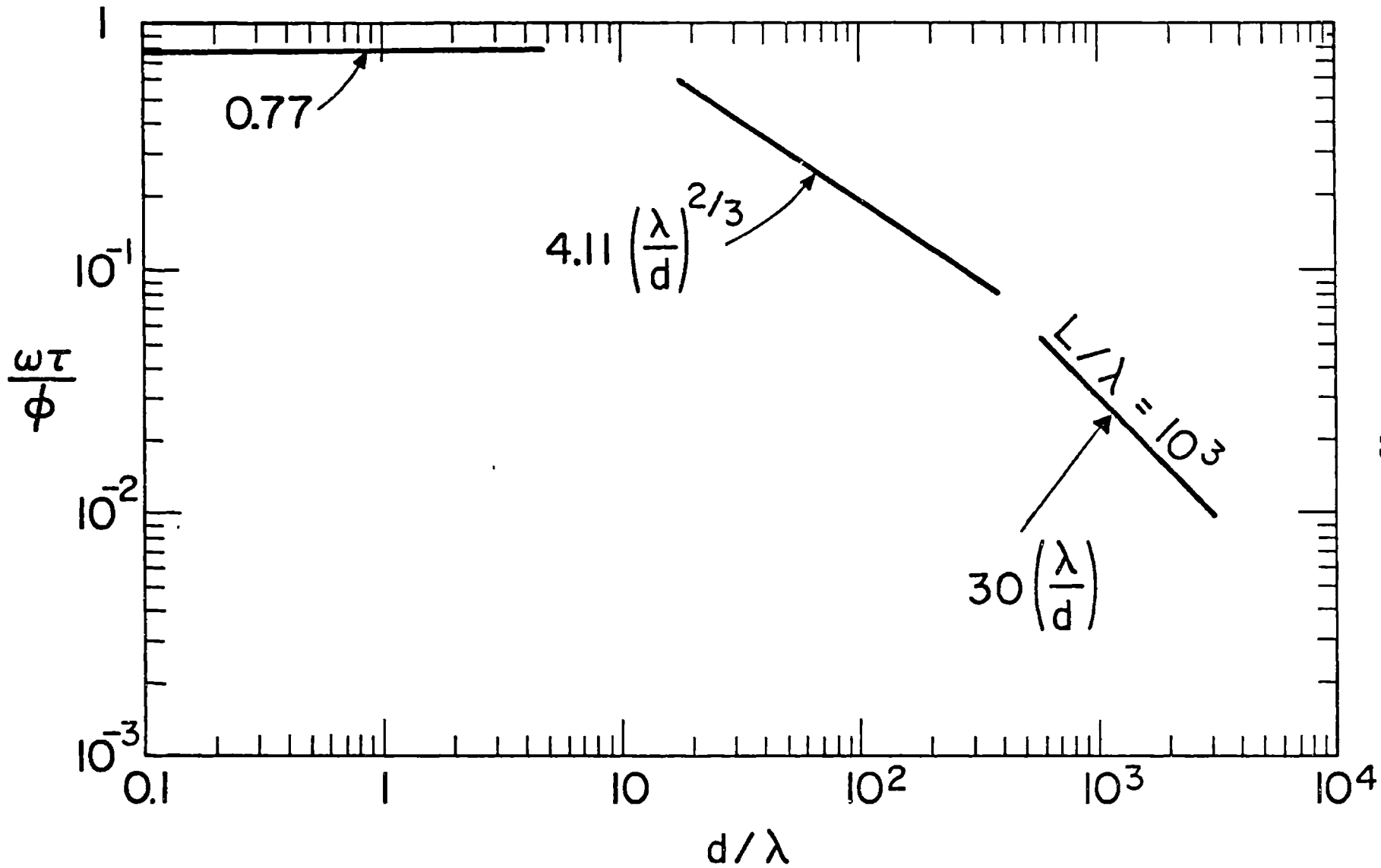


Fig. 2 Theoretical reduced coagulation rate between particles in isotropic turbulent flows as a function of the ratio of the particle size to the Kolmogorov microscale.

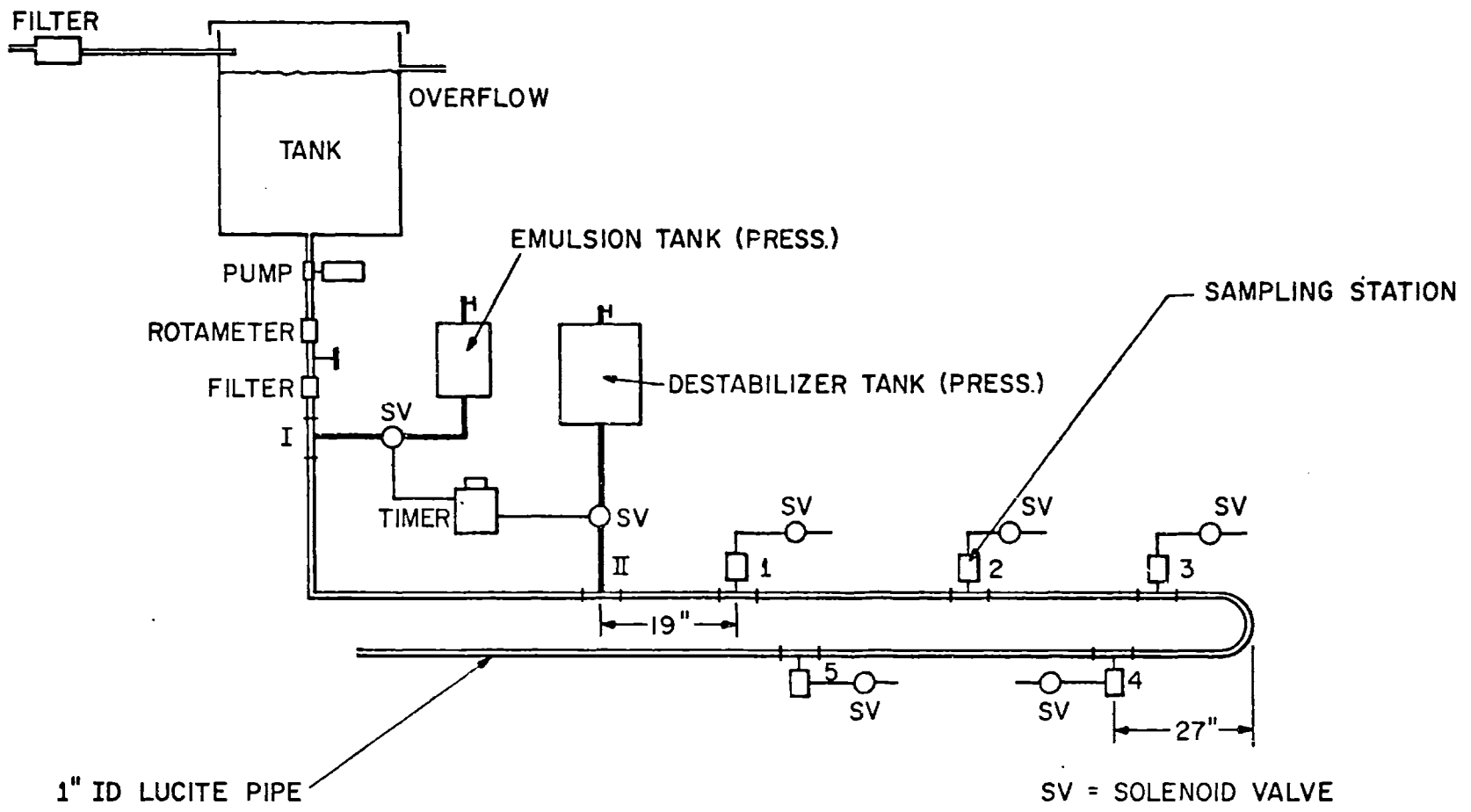


Fig. 3 Experimental setup.

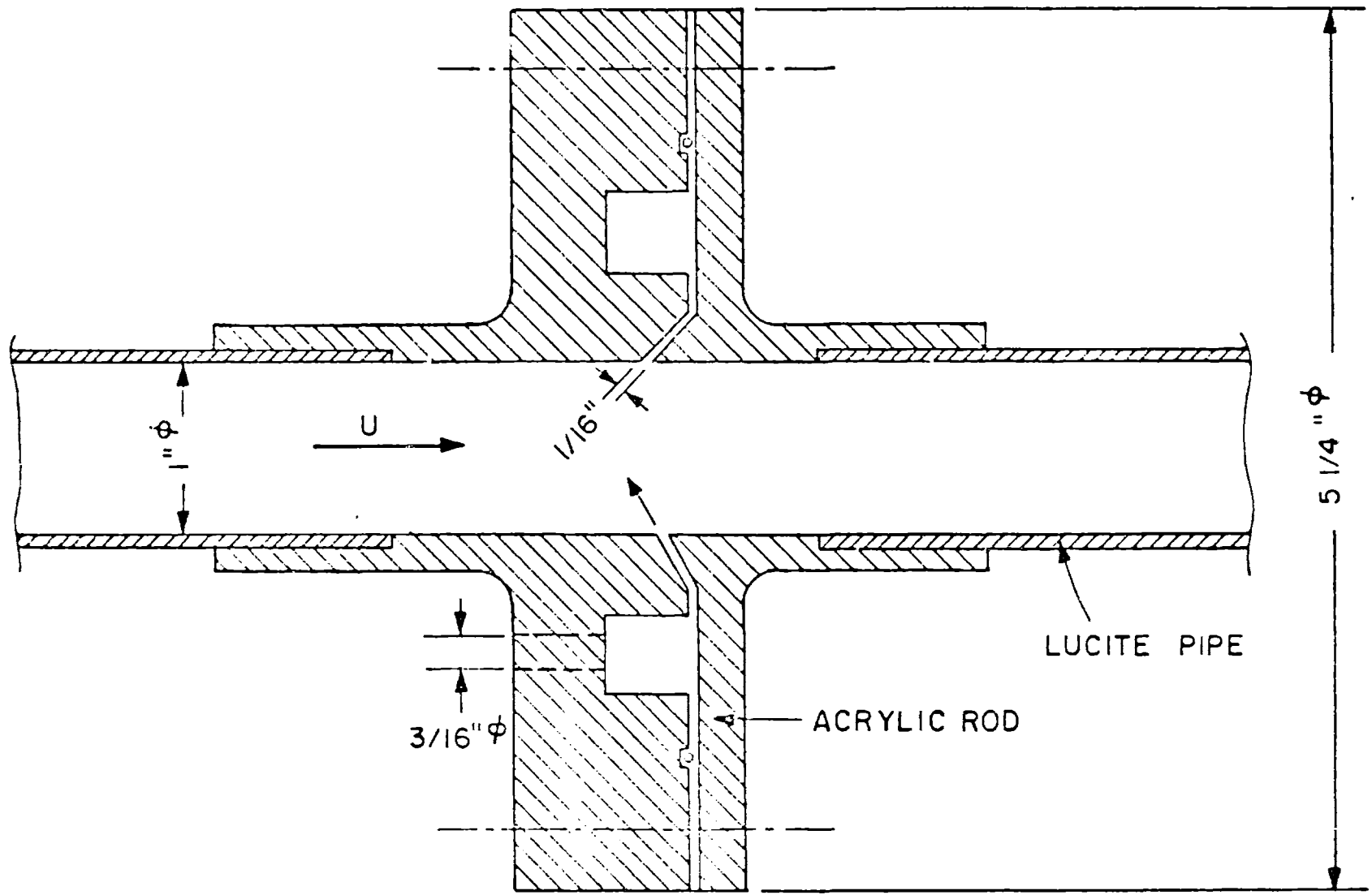


Fig. 4 Destabilizer injection port .

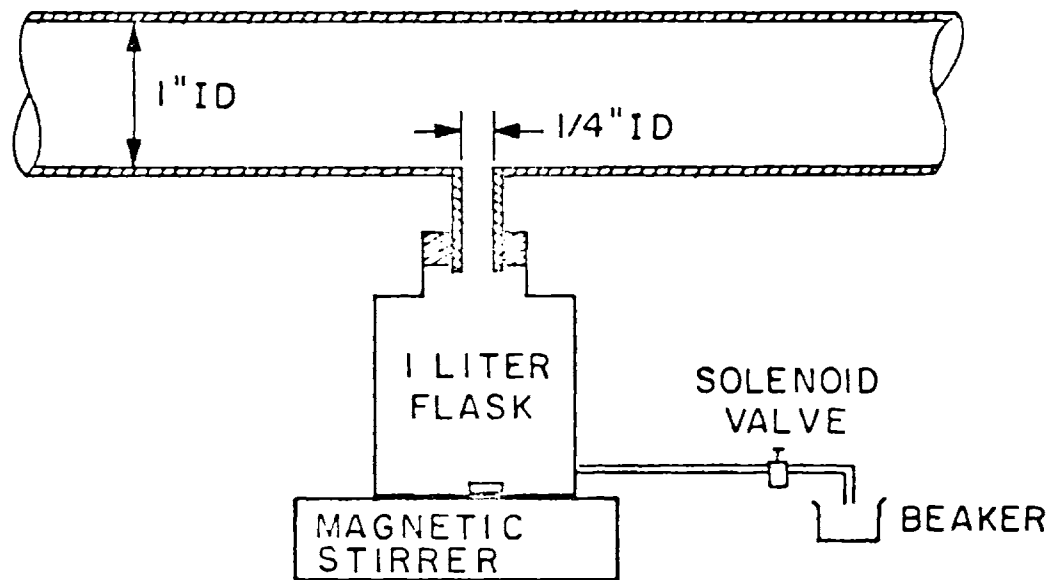


Fig. 5 Typical sampling station.

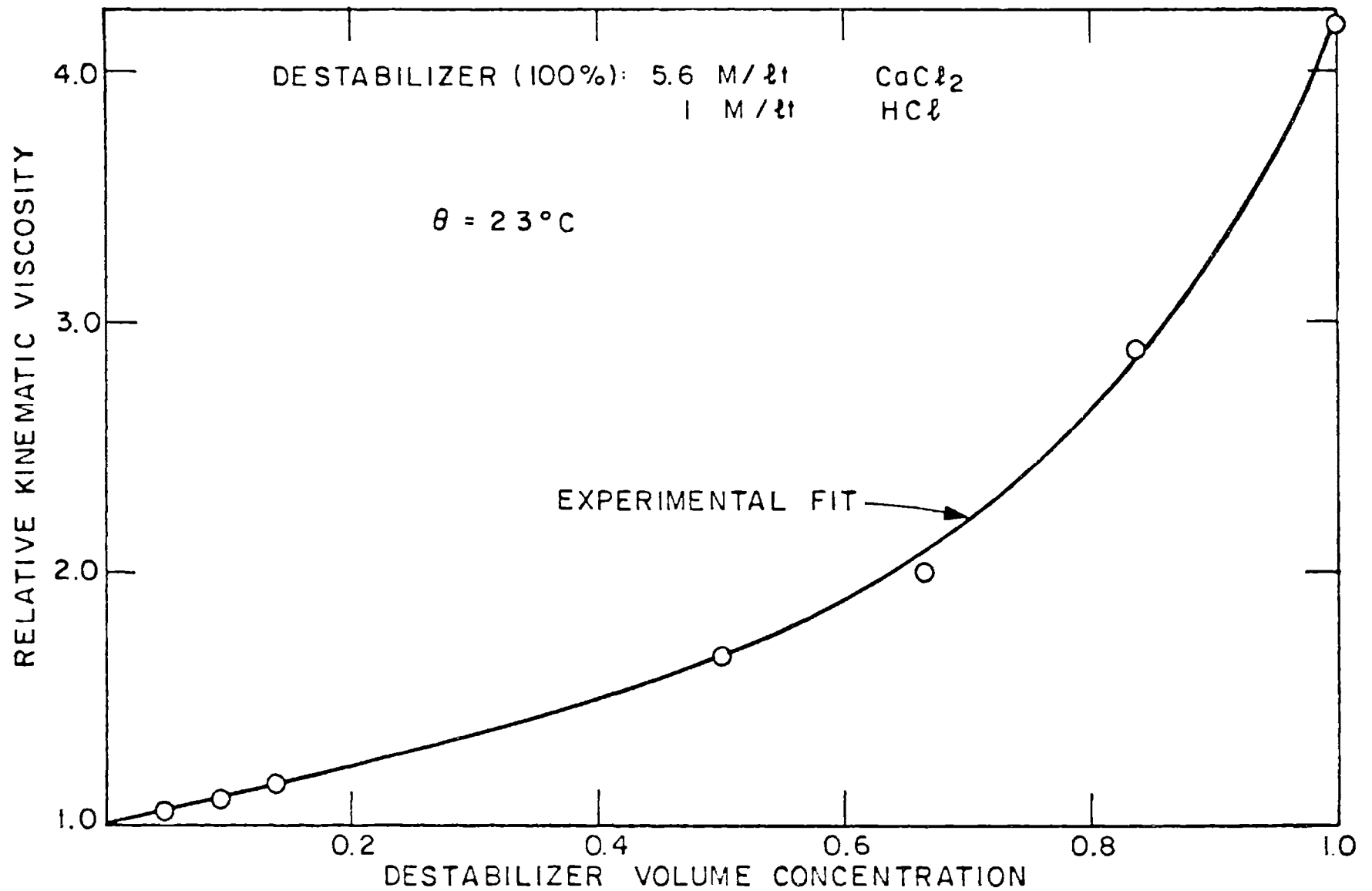


Fig. 6 Kinematic viscosity of the continuous phase vs. the volumetric destabilizer concentration .

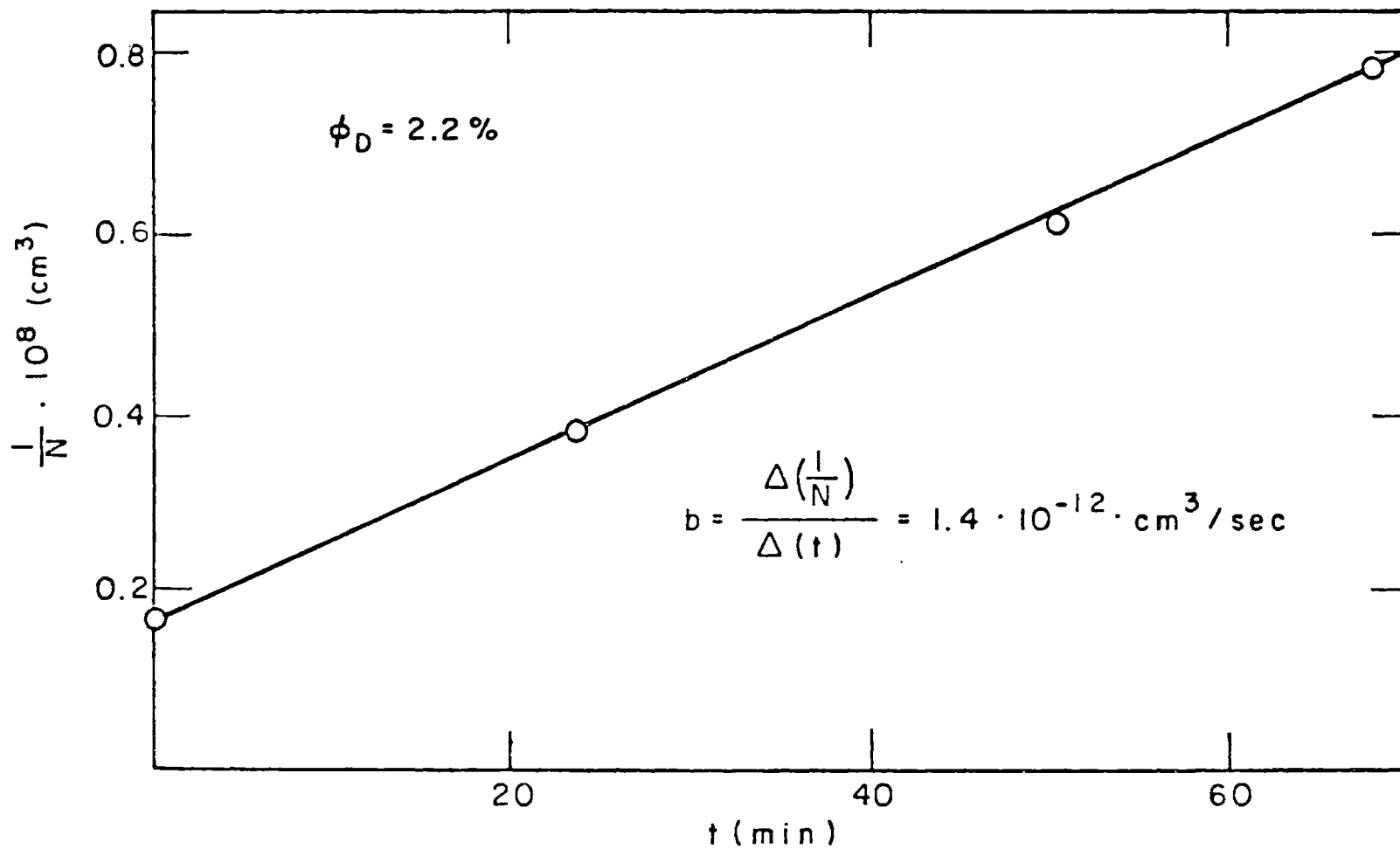


Fig. 7 Inverse particle number density vs. time from the beginning of the Brownian coagulation ($\phi_D = 2.2\%$).

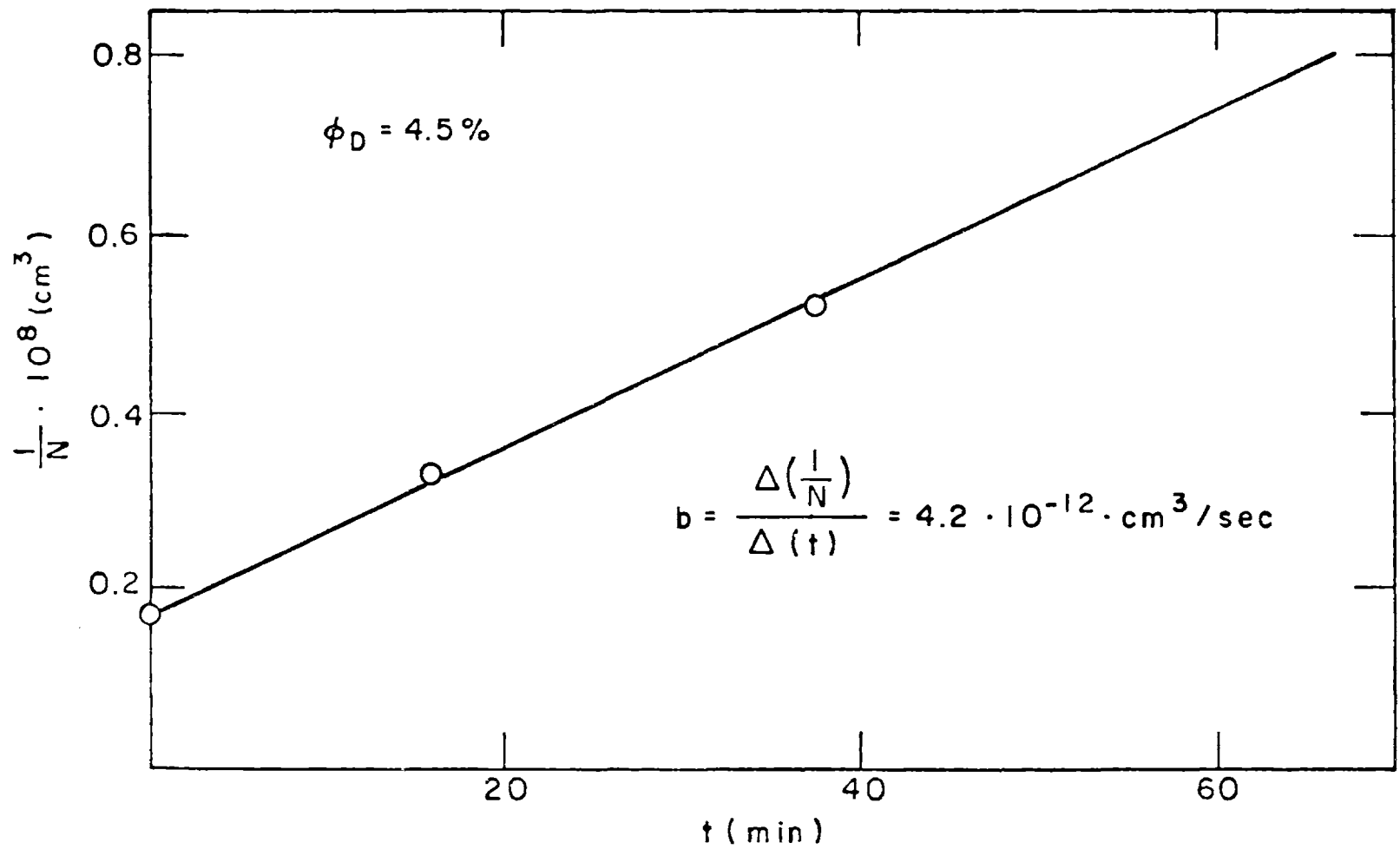


Fig. 8 Inverse particle number density vs. time from the beginning of the Brownian coagulation ($\phi_D = 4.5\%$).

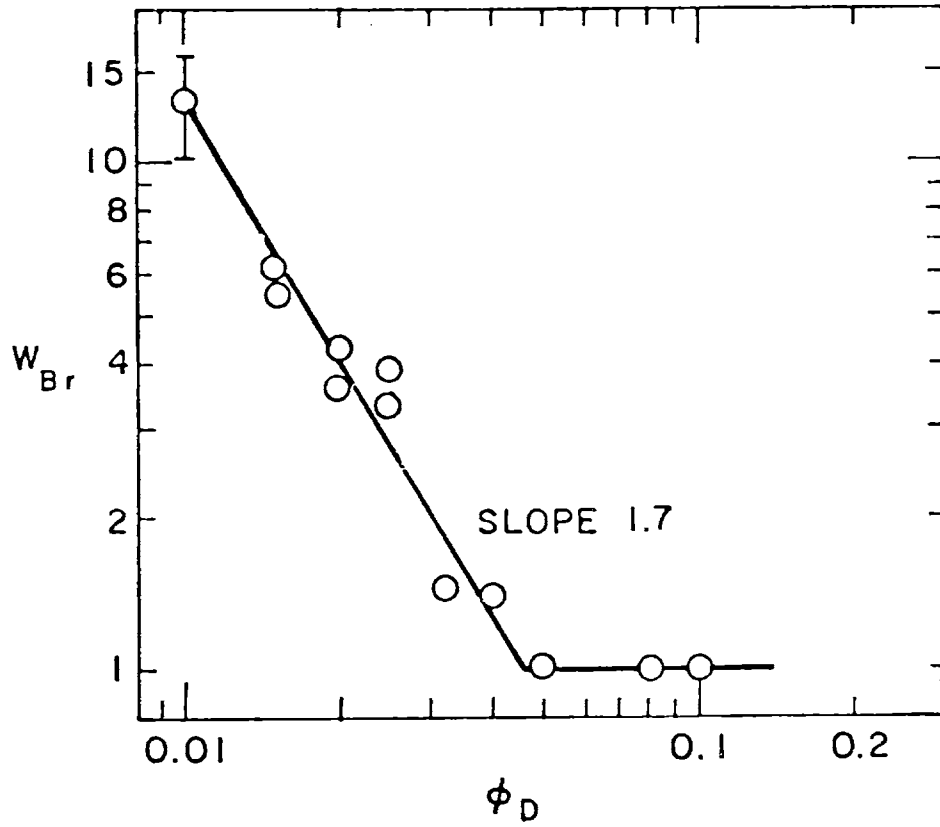


Fig. 9 Stability factor as a function of destabilizer concentration in Brownian coagulation.

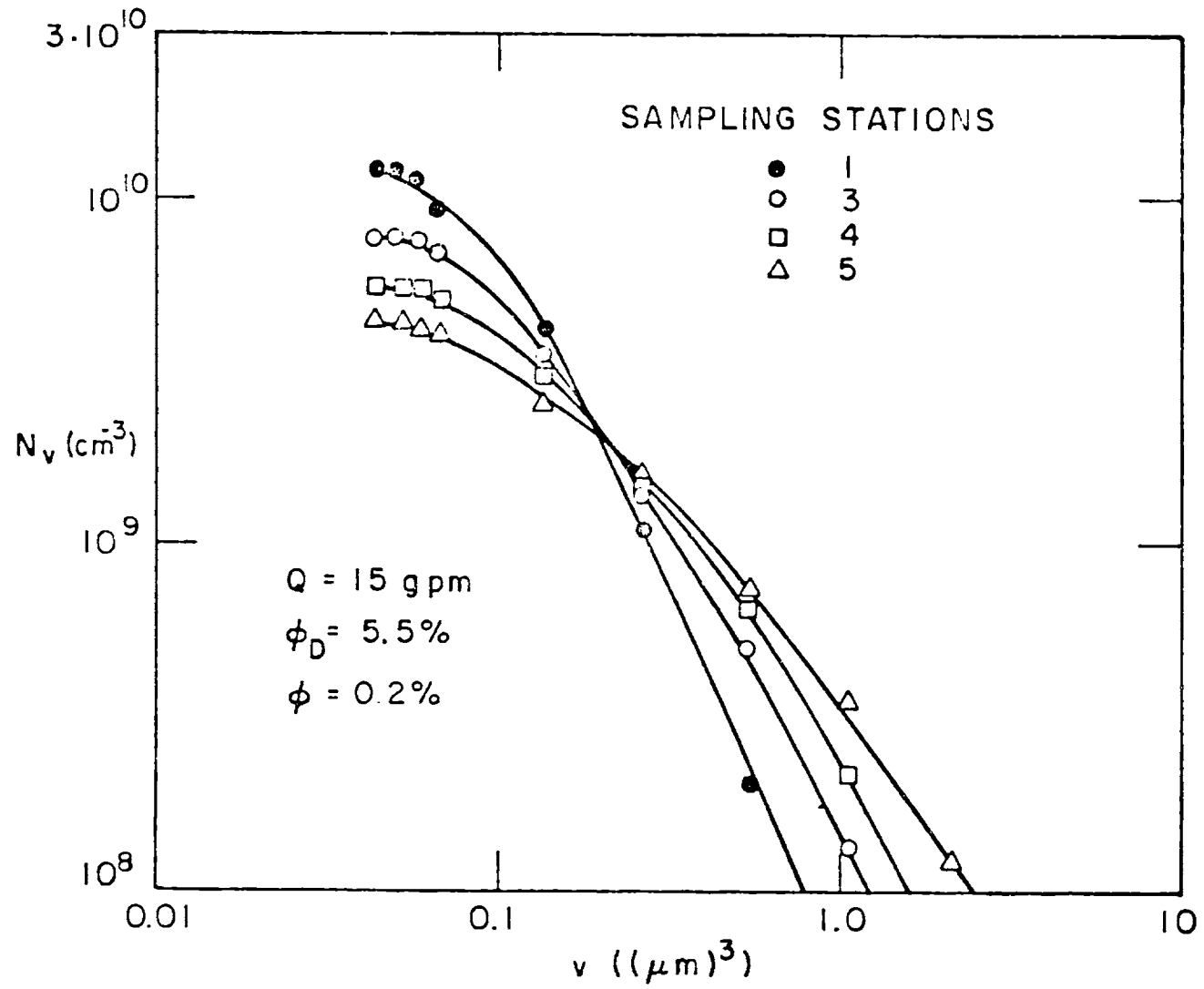


Fig. 10 Cumulative particle size distribution at different sampling stations along the pipe.

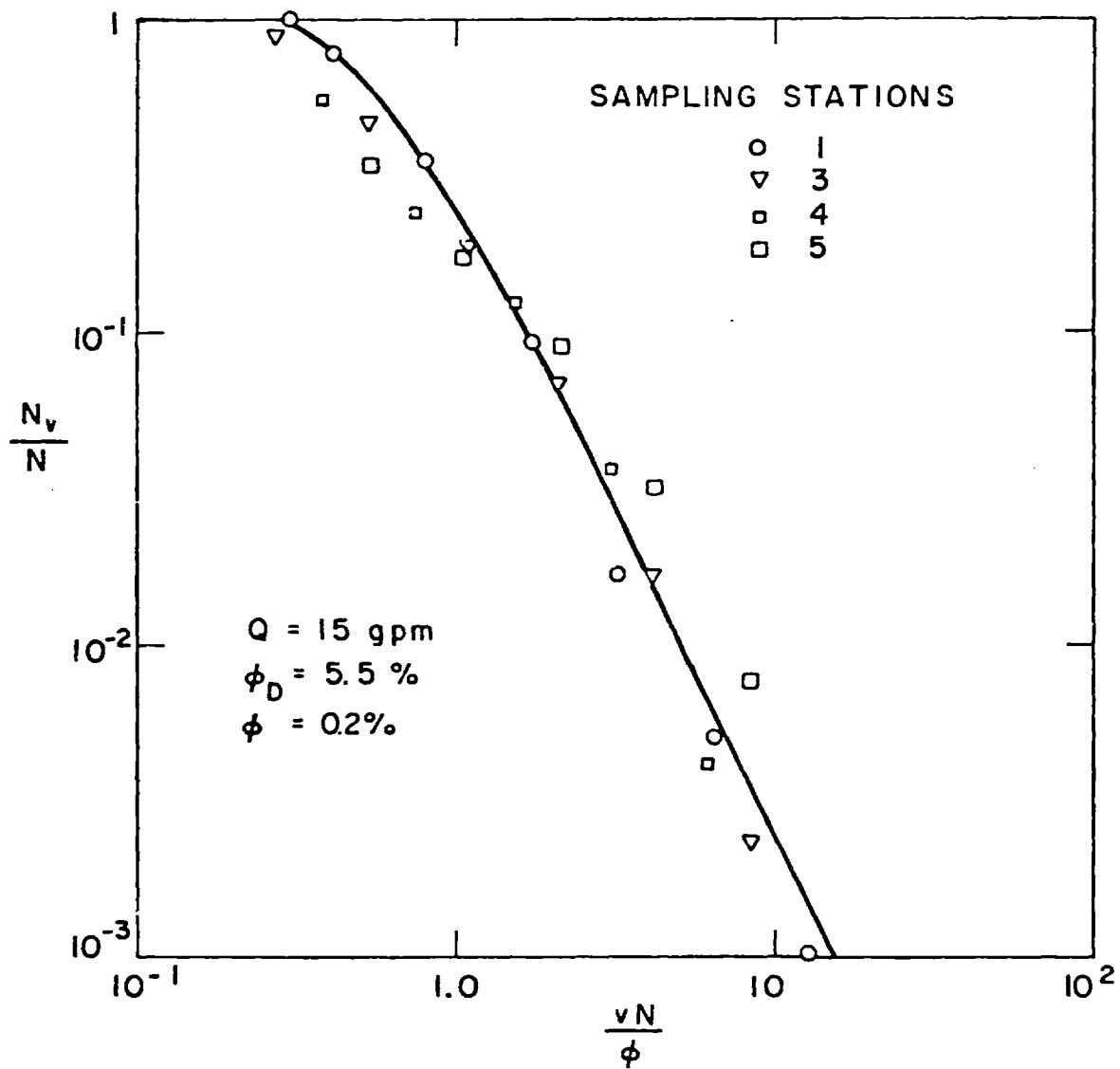


Fig. 11 Cumulative particle size distribution at different sampling stations along the pipe in reduced similarity variables.

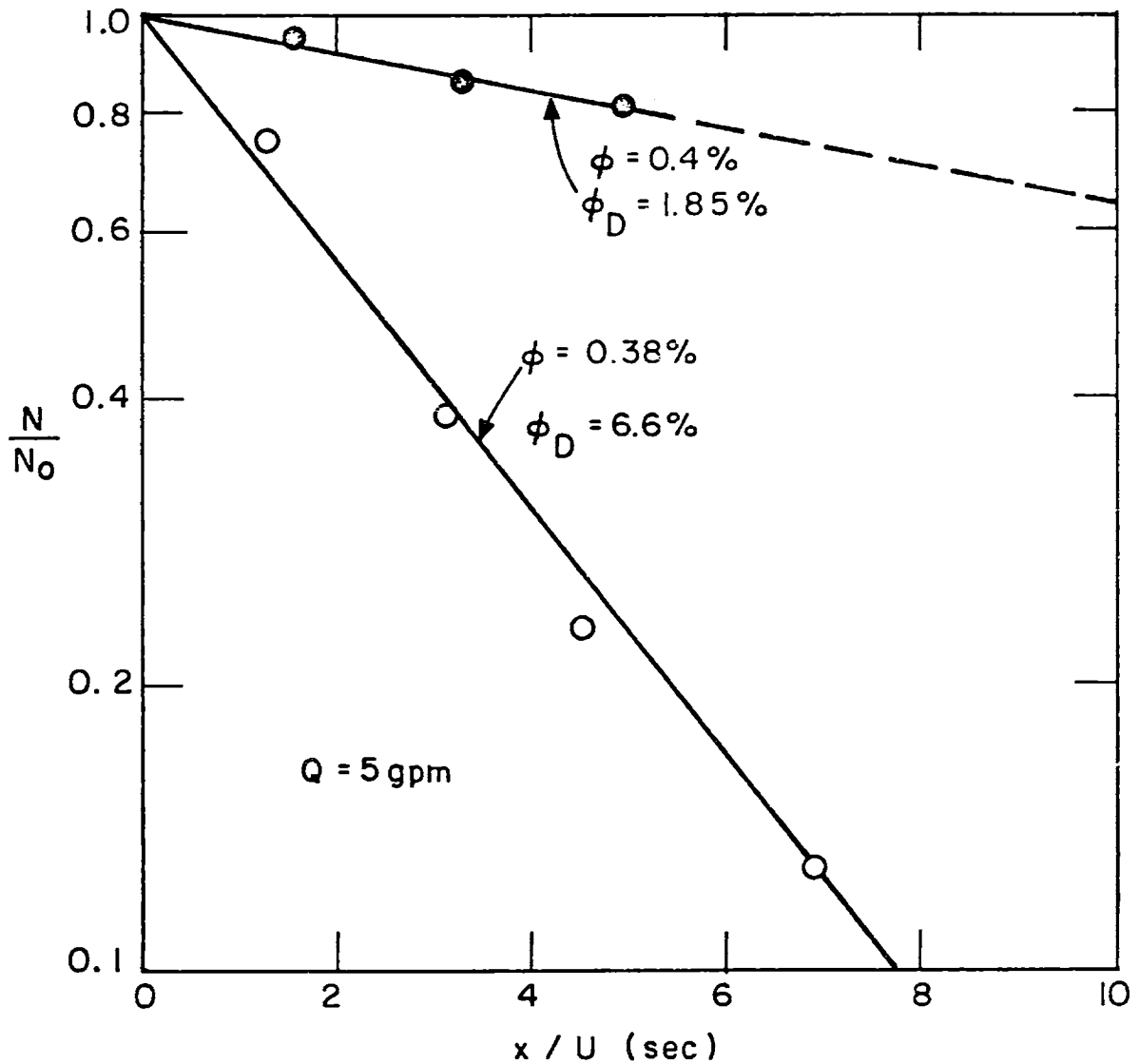


Fig. 12 Particle number density relative to value at first station as a function of distance along the pipe measured in time for dispersion to flow to sampling station ($Q = 5$ gpm).

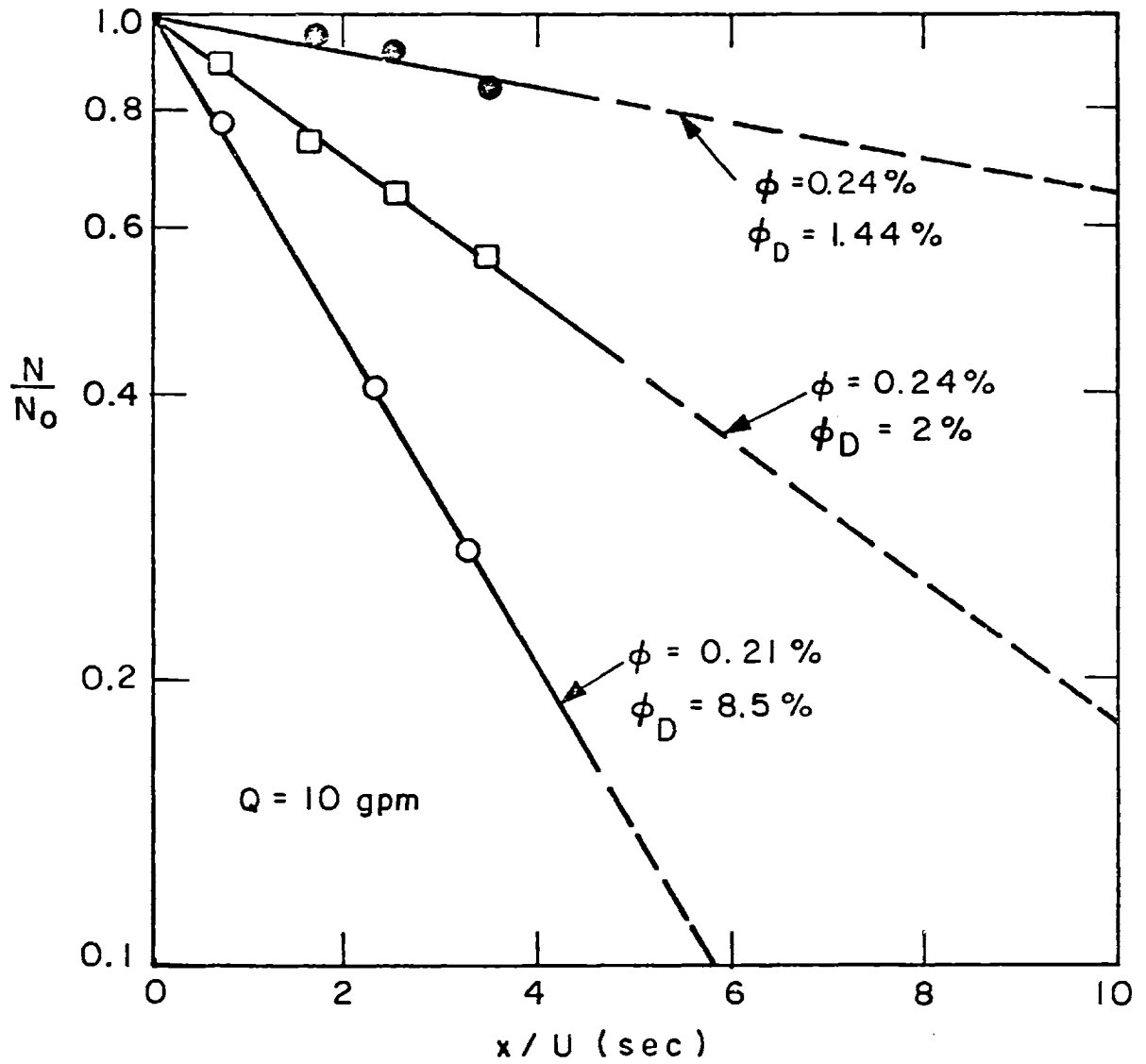


Fig. 13 Particle number density relative to value at first station as a function of distance along the pipe measured in time for dispersion to flow to sampling station ($Q = 10$ gpm).

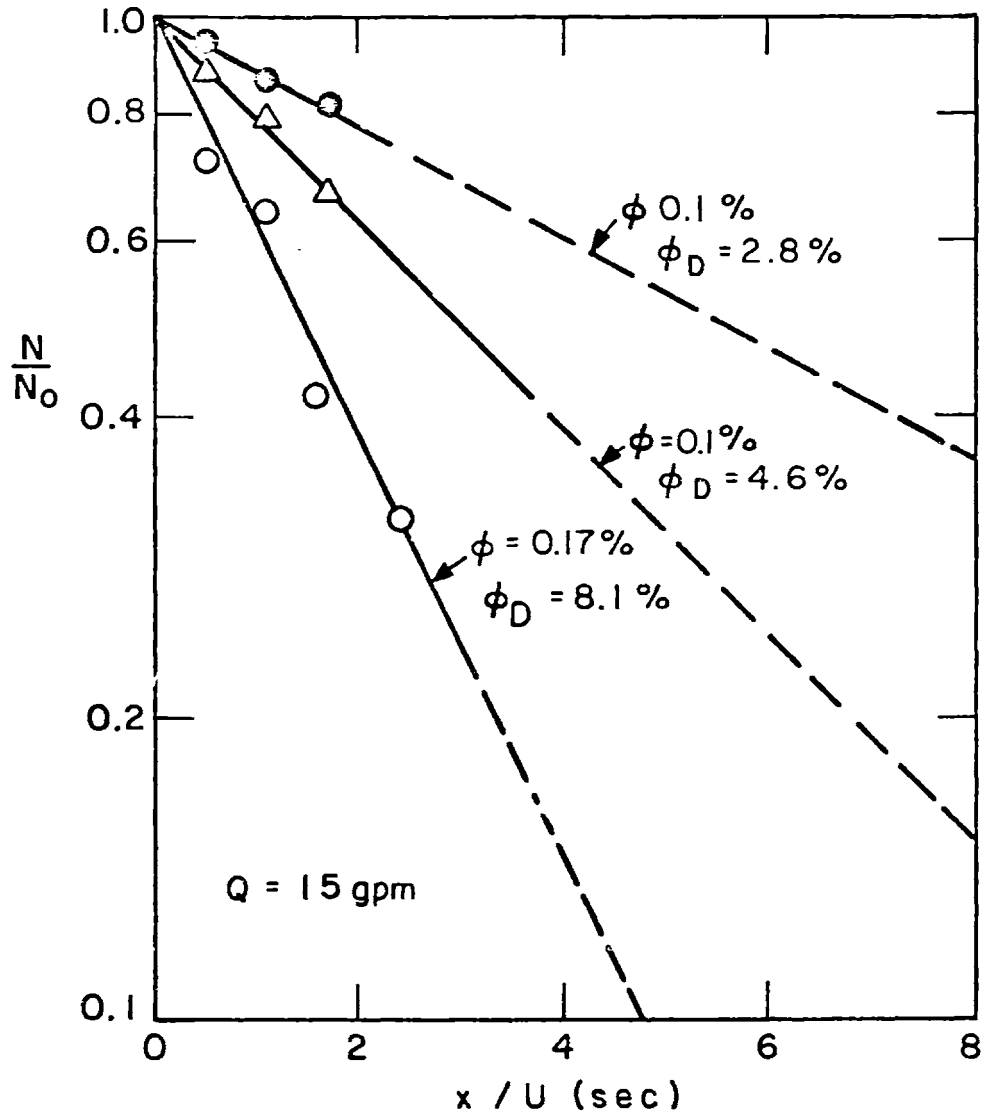


Fig. 14 Particle number density relative to value at first station as a function of distance along the pipe measured in time for dispersion to flow to sampling station ($Q = 15$ gpm).

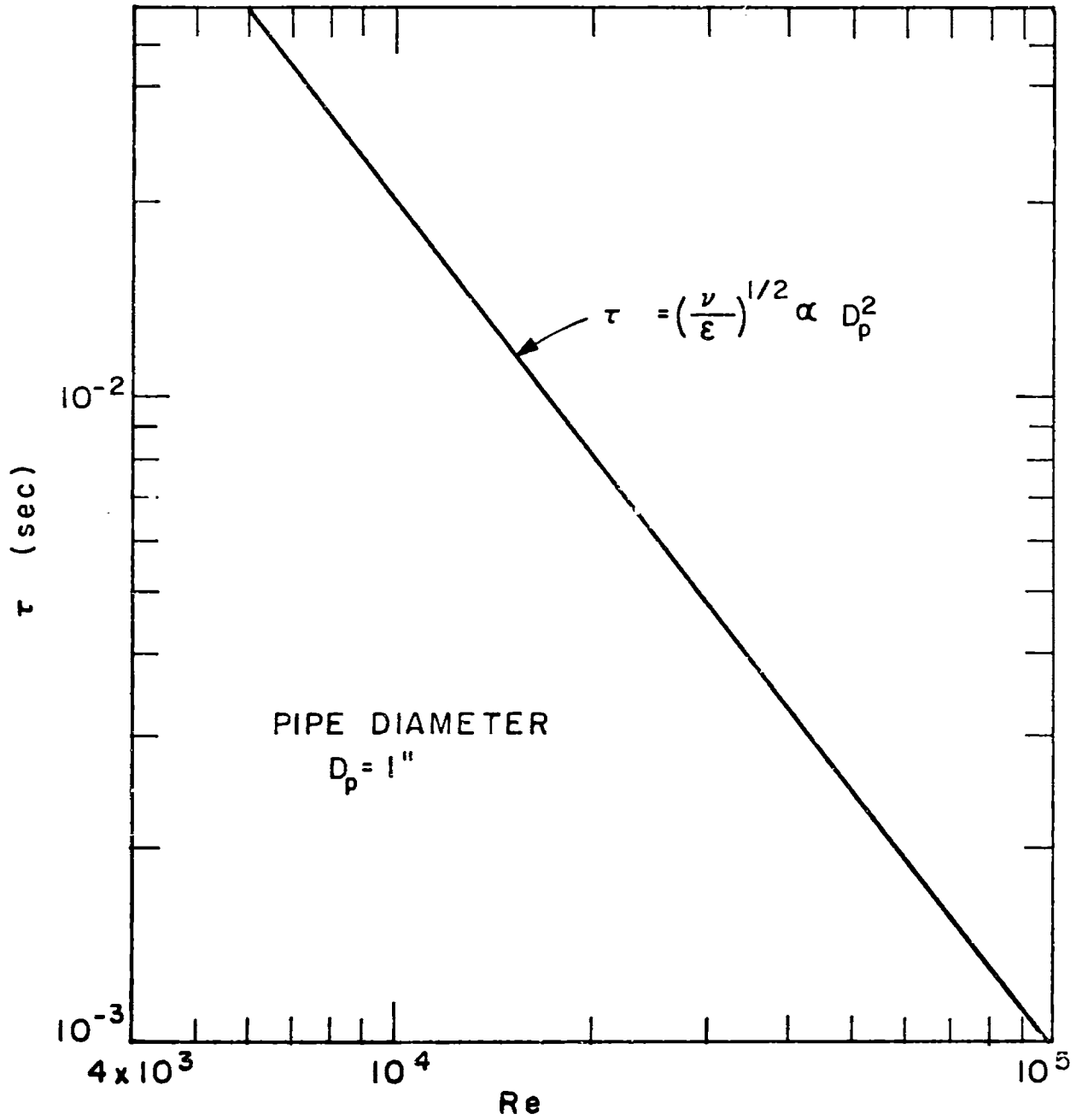


Fig. 15 Kolmogorov time scale vs. Reynolds number in the core of turbulent pipe flows.

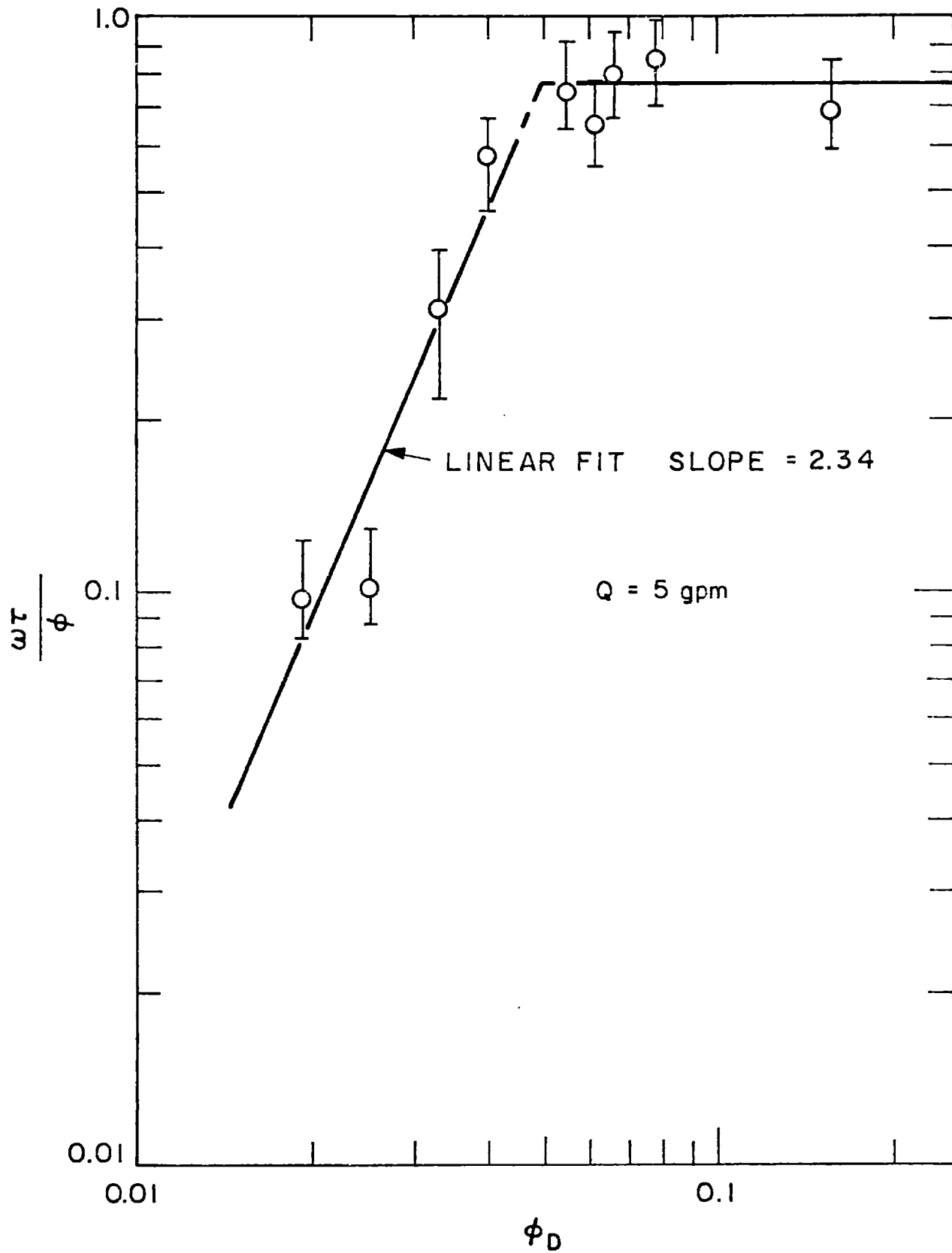


Fig. 16 Measured coagulation rate vs. destabilizer concentration (Q = 5 gpm).

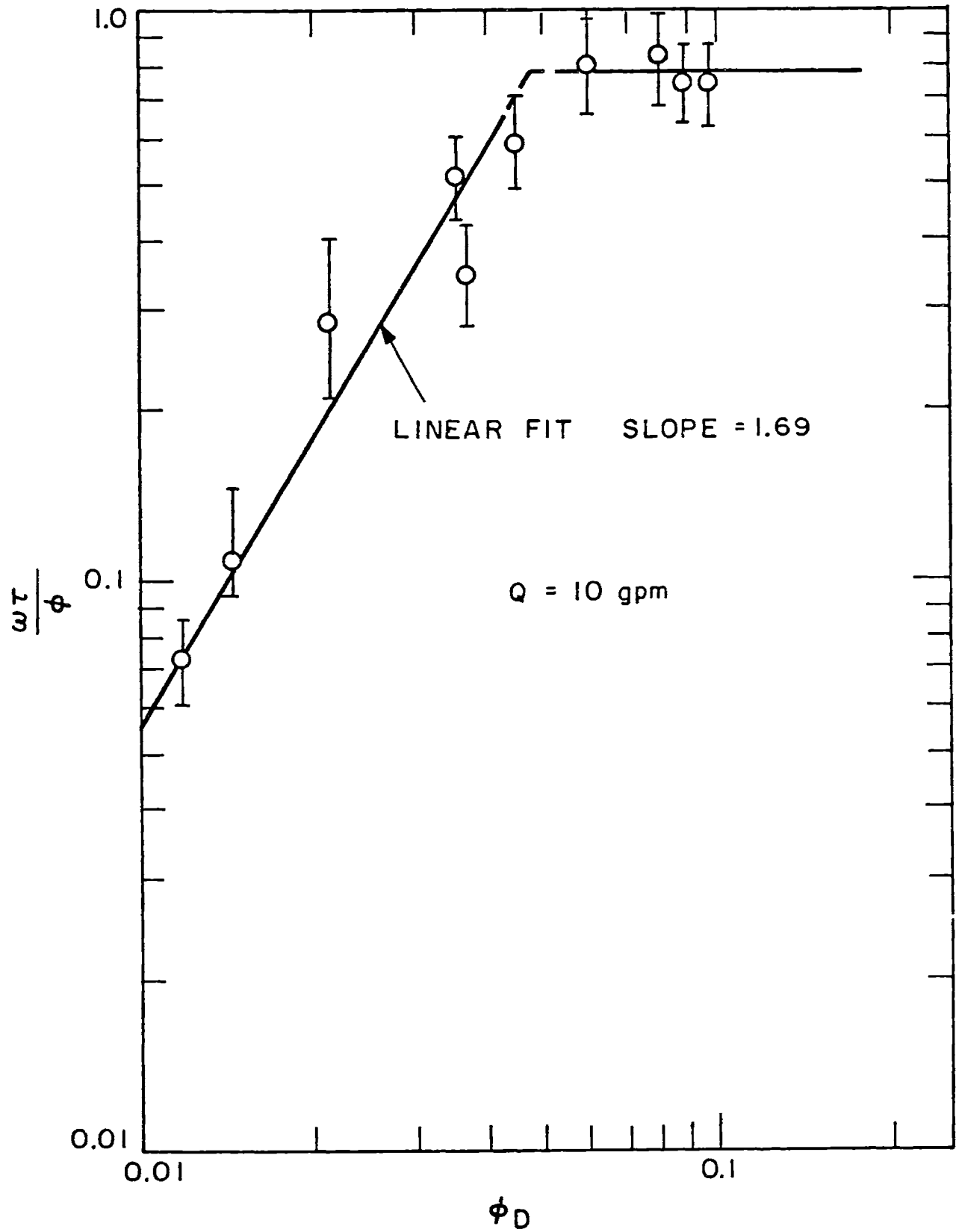


Fig. 17 Measured coagulation rate vs. destabilizer concentration (Q = 10 gpm).

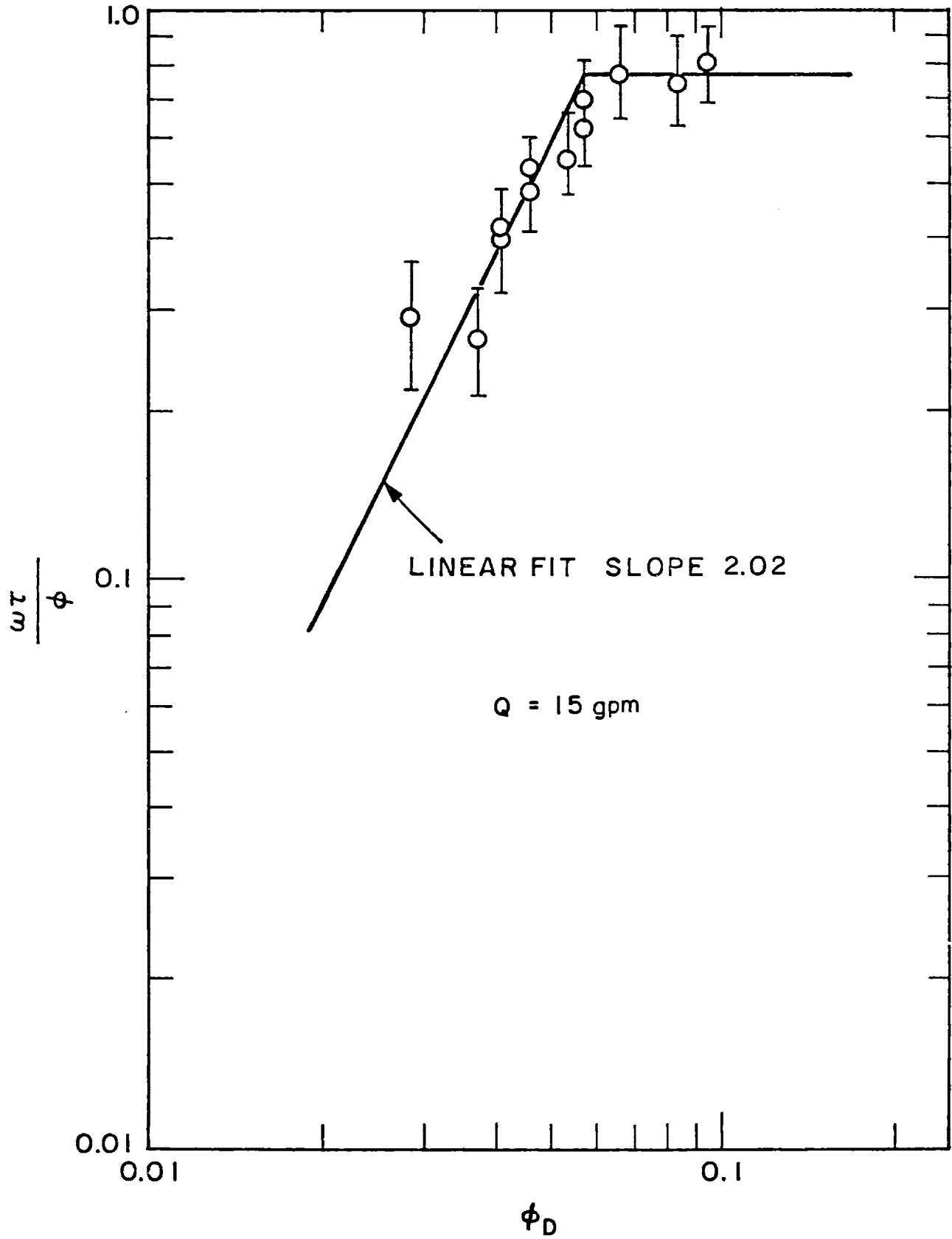


Fig. 18 Measured coagulation rate vs. destabilizer concentration (Q = 15 gpm).

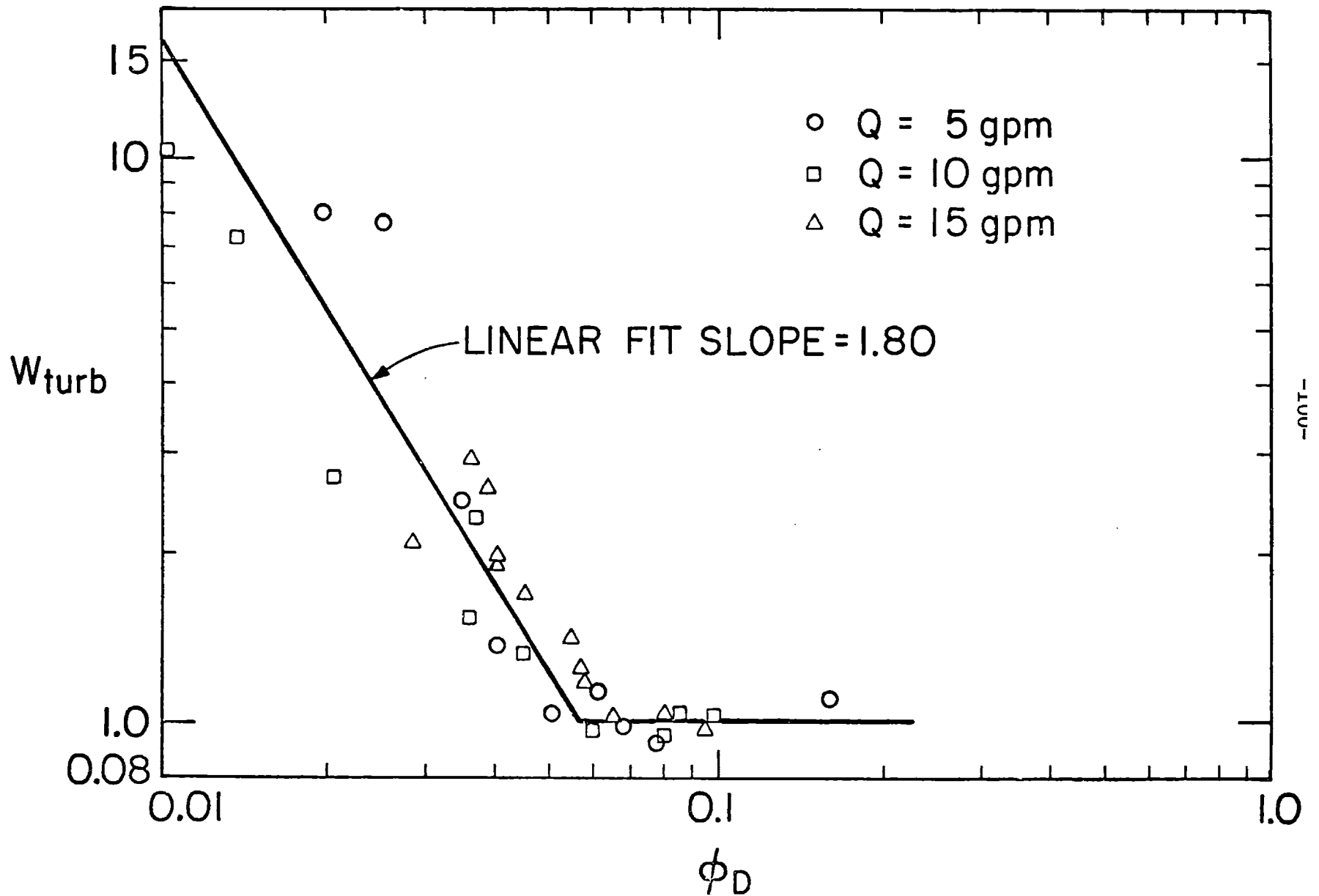


Fig. 19 Stability factor as a function of the destabilizer concentration in turbulent pipe flow coagulation.

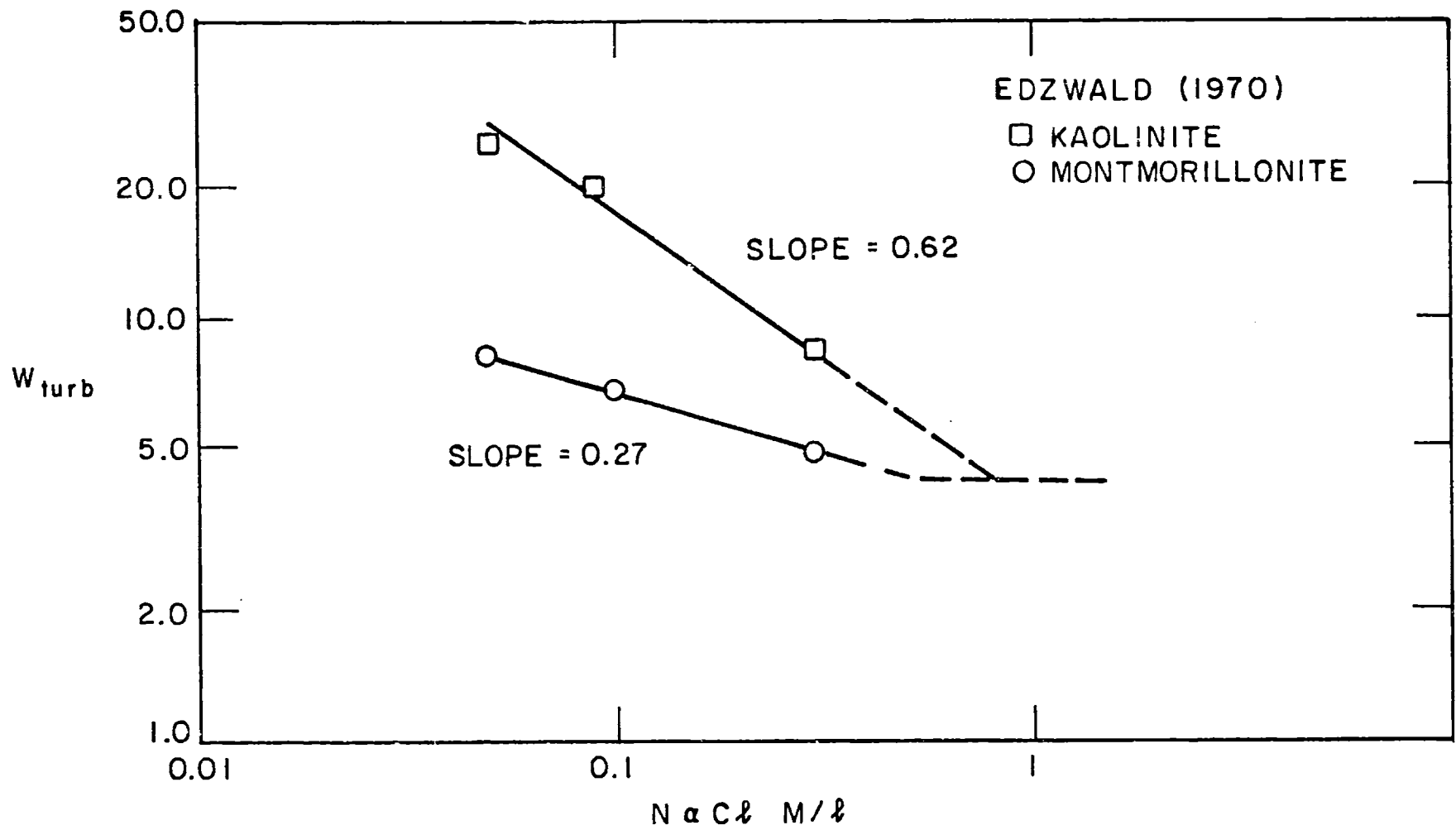


Fig. 20 Stability factor vs. destabilizer concentration in turbulent flows inside agitator tanks.

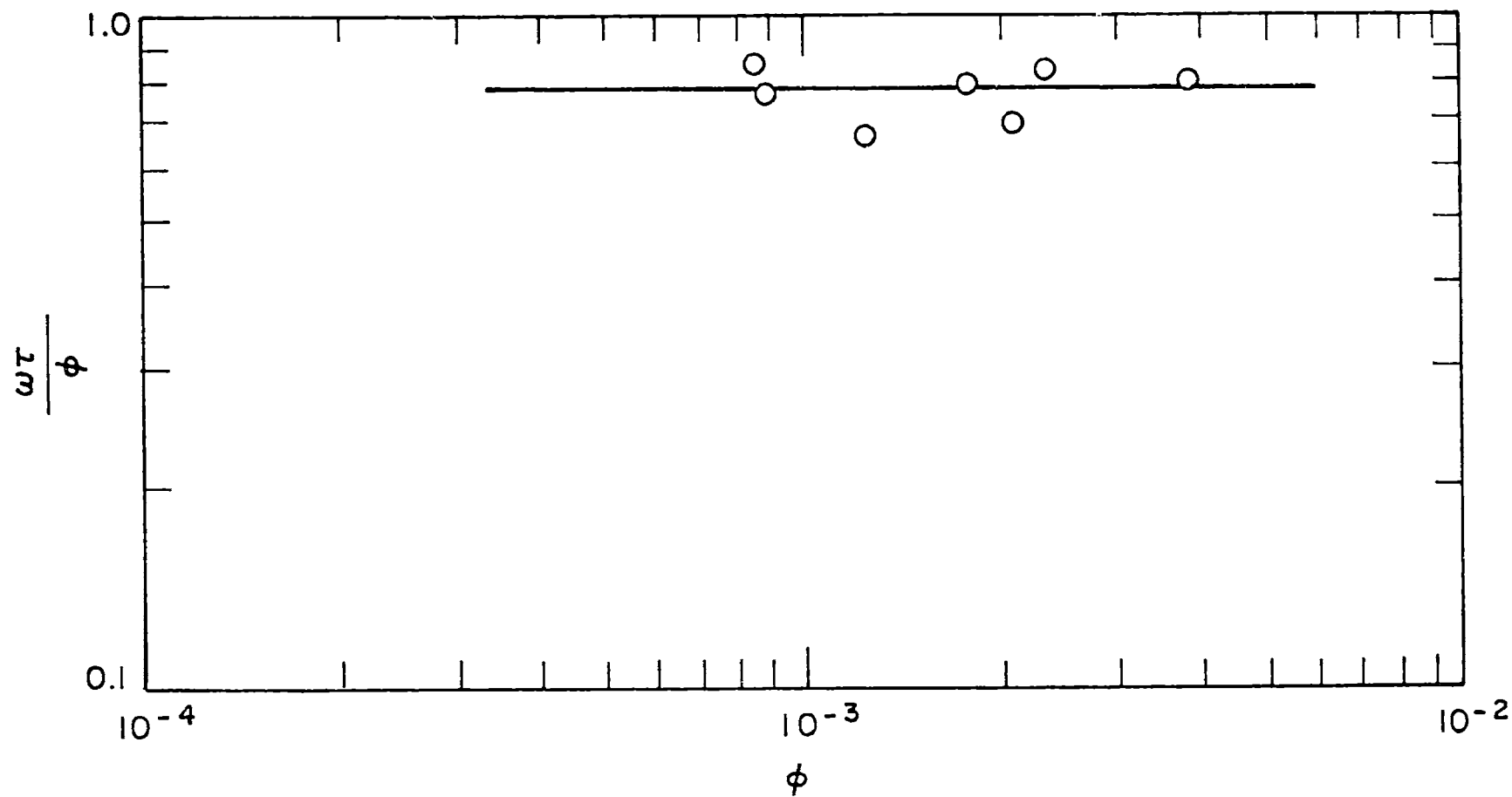
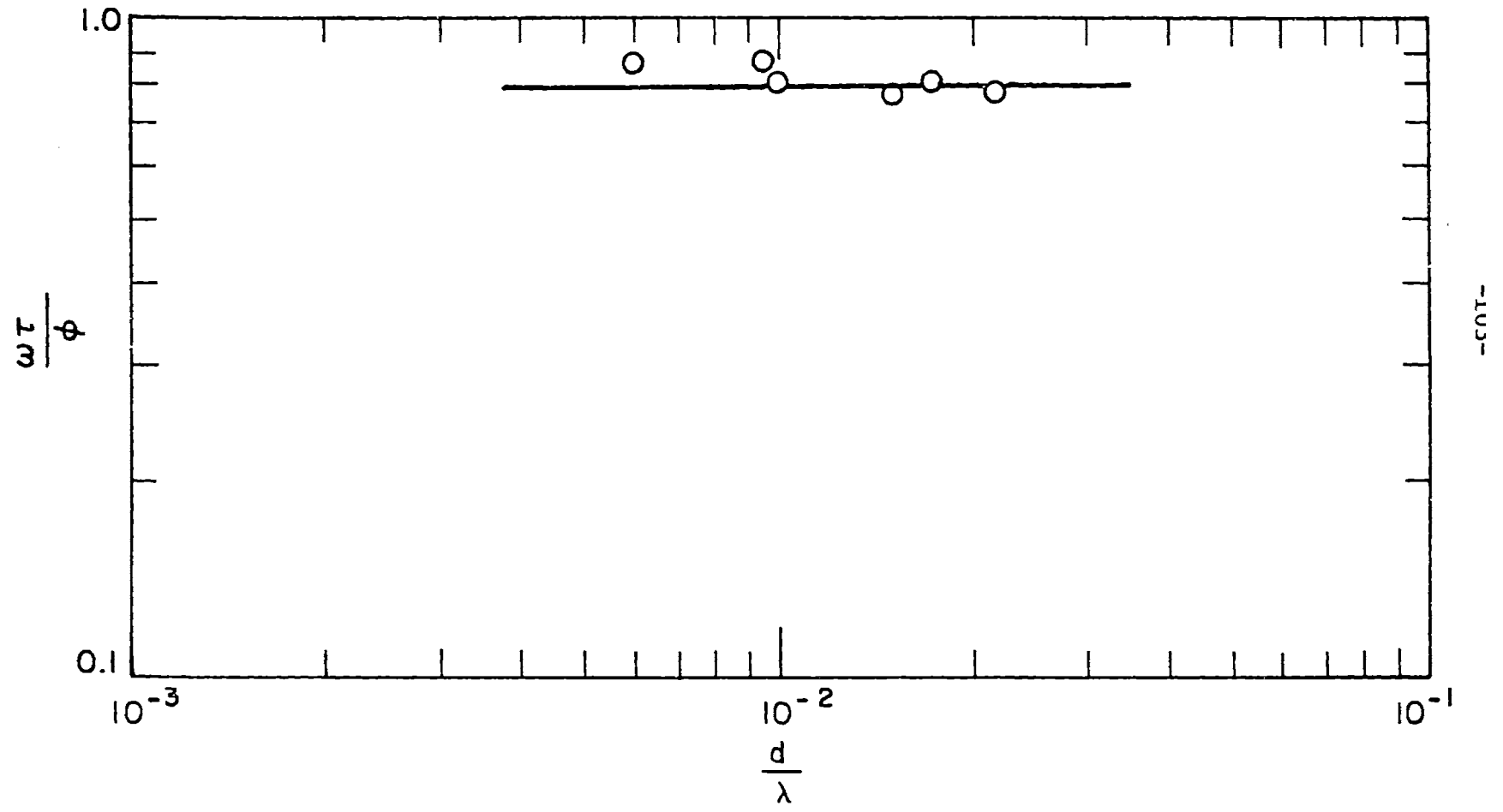


Fig. 21 Measured coagulation rate vs. the volume fraction of the dispersed particles in fully destabilized systems.



-CONT-

Fig. 22 Measured coagulation rate vs. the ratio of the particle size to the Kolmogorov microscale in fully destabilized systems.

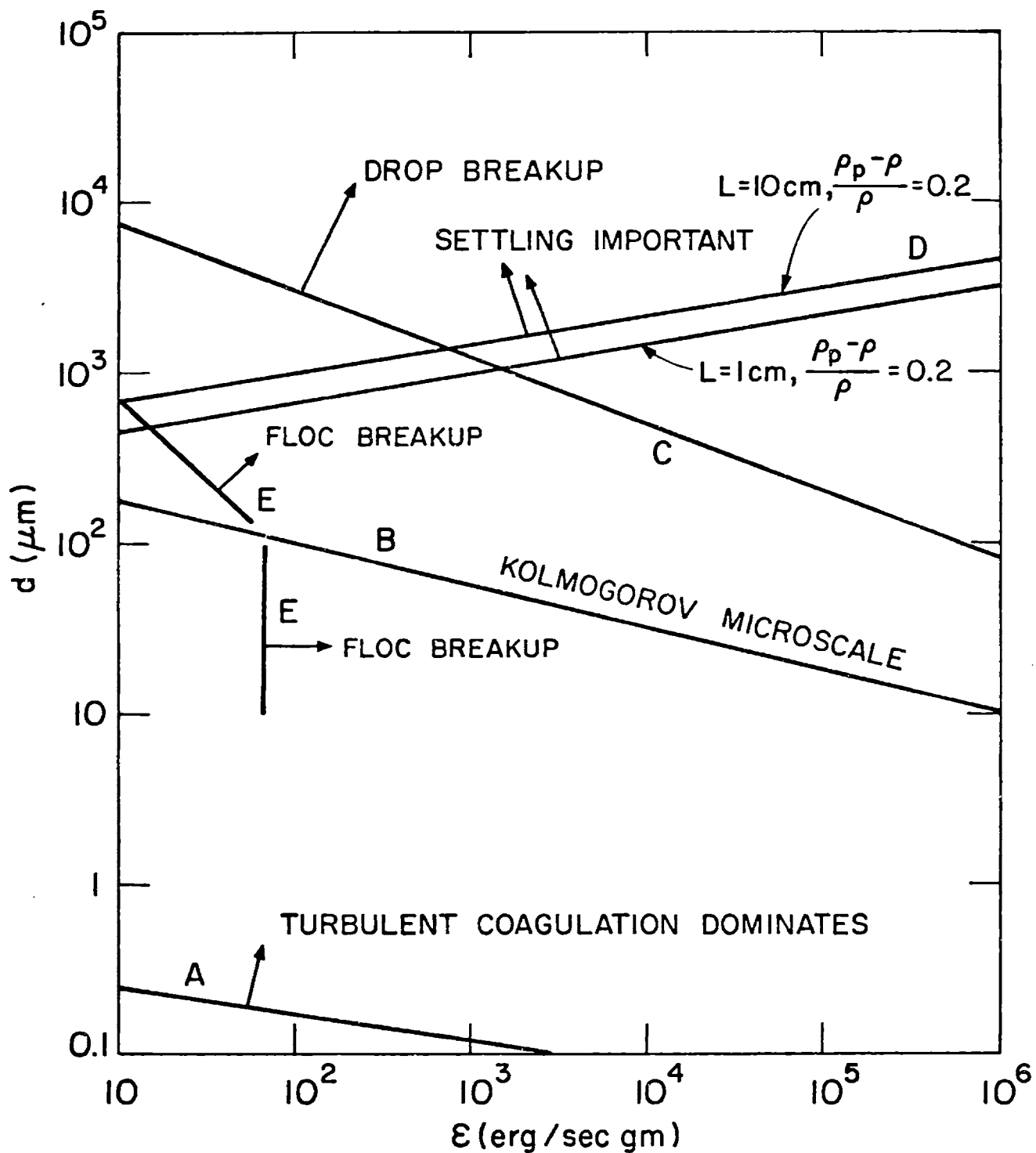


Fig. 23 Particle size vs. the rate of turbulent energy dissipation per unit mass in wastewater treatment systems employing coagulation and sedimentation.

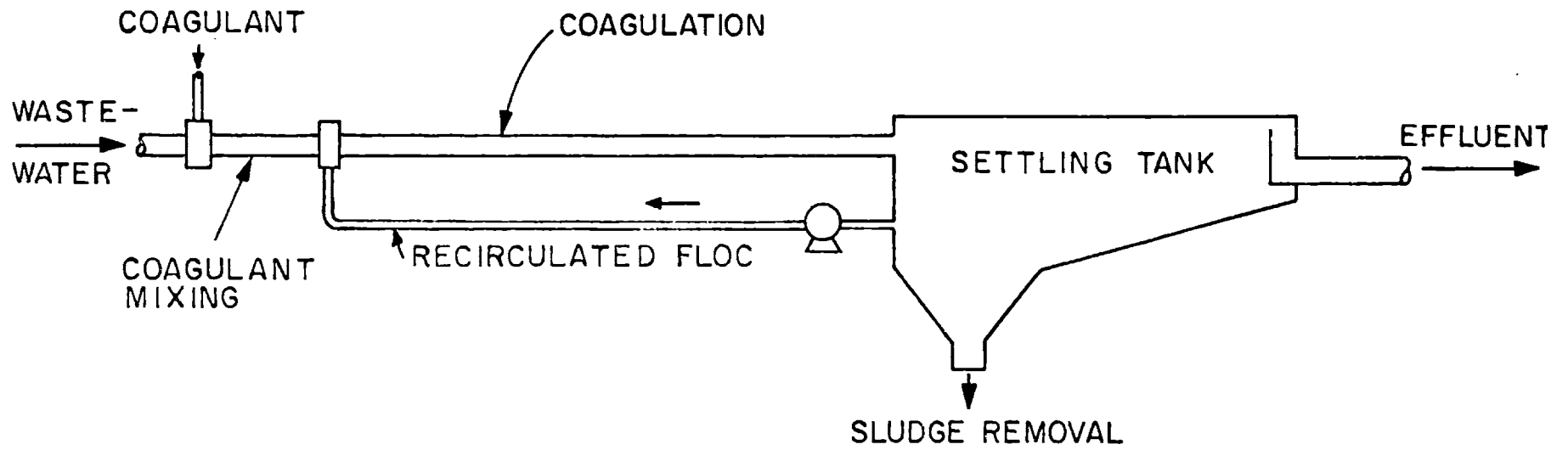


Fig. 24 A new approach to wastewater treatment employing turbulent pipe flow coagulation.

BIOGRAPHICAL NOTE

The author was born January 11, 1945, in Kastoria, Greece. He received his high school diploma from Varvakion High School, Athens, Greece (1962); he ranked first in the entrance examinations to the Mechanical Engineering Department of the National Technical University of Athens (1962); he received his Mechanical Engineering Diploma with highest distinction in the National Technical University of Athens (1967) and his S. M. degree from the Massachusetts Institute of Technology (1971). While an undergraduate, the author was recipient of a Greek Federal scholarship.